ISSN 1905-9094

GMSARN
INTERNATIONAL JOURNAL



Vol. 9 No. 2
June 2015

Published by the

GREATER MEKONG SUBREGION ACADEMIC AND RESEARCH NETWORK
c/o Asian Institute of Technology
P.O. Box 4, Klong Luang, Pathumthani 12120, Thailand

GMSARN INTERNATIONAL JOURNAL

GMSARN MEMBERS

Asian Institute of Technology	P.O. Box 4, Klong Luang, Pathumthani 12120, Thailand. www.ait.asia
Guangxi University	100, Daxue Road, Nanning, Guangxi, CHINA www.gxu.edu.cn
Hanoi University of Science and Technology	No. 1, Daicoviet Street, Hanoi, Vietnam S.R. www.hust.edu.vn
Ho Chi Minh City University of Technology	268 Ly Thuong Kiet Street, District 10, Ho Chi Minh City, Vietnam. www.hcmut.edu.vn
Institute of Technology of Cambodia	BP 86 Blvd. Pochentong, Phnom Penh, Cambodia. www.itc.edu.kh
Khon Kaen University	123 Mittraparb Road, Amphur Muang, Khon Kaen, Thailand. www.kku.ac.th
Kunming University of Science and Technology	121 Street, Kunming P.O. 650093, Yunnan, China. www.kmust.edu.cn
Nakhon Phanom University	330 Apibanbuncha Road, Nai Muang Sub-District, Nakhon Phanom 48000, THAILAND www.npu.ac.th
National University of Laos	P.O. Box 3166, Vientiane Perfecture, Lao PDR. www.nuol.edu.la
Royal University of Phnom Penh	Russian Federation Blvd, PO Box 2640 Phnom Penh, Cambodia. www.rupp.edu.kh
Thammasat University	P.O. Box 22, Thamamasat Rangsit Post Office, Bangkok 12121, Thailand. www.tu.ac.th
Ubon Ratchathani University	85 Sathollmark Rd. Warinchamrap Ubon Ratchathani 34190, THAILAND www.ubu.ac.th
Yangon Technological University	Gyogone, Insein P.O. Yangon, Myanmar www.most.gov.mm/ytu/
Yunnan University	2 Cuihu Bei Road Kunming, 650091, Yunnan Province, China. www.ynu.edu.cn

ASSOCIATE MEMBER

Mekong River Commission	P.O. Box 6101, Unit 18 Ban Sithane Neua, Sikhottabong District, Vientiane 01000, LAO PDR www.mrcmekong.org

GMSARN
INTERNATIONAL JOURNAL

GREATER MEKONG SUBREGION ACADEMIC AND RESEARCH NETWORK (http://www.gmsarn.com)

The Greater Mekong Subregion (GMS) consists of Cambodia, China (Yunnan & Guangxi Provinces), Laos, Myanmar, Thailand and Vietnam.

The Greater Mekong Subregion Academic and Research Network (GMSARN) was founded followed an agreement among the founding GMS country institutions signed on 26 January 2001, based on resolutions reached at the Greater Mekong Subregional Development Workshop held in Bangkok, Thailand, on 10 - 11 November 1999. GMSARN was composed of eleven of the region's top-ranking academic and research institutions. GMSARN carries out activities in the following areas: human resources development, joint research, and dissemination of information and intellectual assets generated in the GMS. GMSARN seeks to ensure that the holistic intellectual knowledge and assets generated, developed and maintained are shared by organizations within the region. Primary emphasis is placed on complementary linkages between technological and socio-economic development issues. Currently, GMSARN is sponsored by Royal Thai Government.

The GMSARN current member institutions are the Asian Institute of Technology, Pathumthani, Thailand; Guangxi University, Guangxi Province, China; Hanoi University of Science and Technology, Hanoi, Vietnam; Ho Chi Minh City University of Technology, Ho Chi Minh City, Vietnam; The Institute of Technology of Cambodia, Phnom Penh, Cambodia; Khon Kaen University, Khon Kaen Province, Thailand; Kunming University of Science and Technology, Yunnan Province, China; Nakhon Phanom University, Nakon Phanom Province, Thailand; National University of Laos, Vientiane, Laos PDR; The Royal University of Phnom Penh, Phnom Penh, Cambodia; Thammasat University, Bangkok, Thailand; Ubon Ratchathani University, Ubon Ratchathani Province, Thailand; Yangon Technological University, Yangon, Myanmar; and Yunnan University, Yunnan Province, China and another associate member is Mekong River Commission, Vientiane, Laos PDR.

GMSARN International Journal

Volume 9, Number 2, June 2015

CONTENTS

Improved Particle Swarm Optimization Method for Optimal Power Flow with Facts Devices

Dinh Luong Le, Dac Loc Ho and Ngoc Dieu Vo

Abstract*— *This paper proposes an Improved Particle Swarm Optimization (IPSO) algorithm for solving optimal power flow with Facts devices problem. Two main types of FACTS devices, namely Static VAR Compensator (SVC) and Thyristor Controlled Series Compensator (TCSC) are applied to the OPF problem. In the new improved method, the conventional IPSO algorithm is used with the variance coefficients to speed up the convergence to the global solution in a fast manner regardless of the shape of the cost function. The proposed IPSO has been tested on various systems with FACTS devices to minimize the total generation fuel cost, investment costs of FACTS devices and keep the power flow within their security limits. The obtained numerical results have shown that the IPSO method is more efficient and faster than many other methods reported in the literature for finding the optimal solution of optimal power flow with Facts devices. Therefore, the proposed IPSO method can be a promising method for solving the practical optimal power flow with Facts devices problems.

***Keywords*— Facts devices; Particle Swarm Optimization; Optimal Power Flow; SVC; TCSC.**

1. INTRODUCTION

Most of the power supply system in the world is linked together broadly to address technical and economic problems. Although the building electrical system based on the load forecast but not always ensure balance between supply and demand. So the power system operating status will have some line-load lines carry some heavy loads. Transmission lines are presented limited by the temperature factor, capacitance and stability. So if not adjusted appropriate transmission lines will not make full use of its power transmission capabilities. Furthermore, because of environmental conditions, line corridor should not easily build new grid system arbitrarily renovate and replace the old system with ease.

Thereby need to reconsider traditional phone systems and implement measures for power distribution to control the power system operation more flexible and reliable. One of the control device is now the world's attention system FACTS Flexible AC [1], it can control the voltage, current, impedance phase angle of the power system, which helps improve stability too high (due to control power flow on effects, resistance, voltage and current level of short-circuit) or the phenomenon of resonance oscillation frequency below).

With the rapid development of power electronics, Flexible AC Transmission Systems (FACTS) devices have been proposed and implemented in power systems. FACTS devices can be used to control power flow and enhance system stability. There is an increasing interest in using FACTS devices in the operation and control of power systems. However, their coordination with the conventional damping controllers in aiding of power system oscillation damping is still an open problem. Therefore, it is essential to investigate the coordinated control of FACTS devices and traditional power system controllers in large power systems.

Recently, appeared PSO algorithm, this algorithm has several advantages compared to other methods of computational time faster and stable convergence [2]. Scientists have applied PSO algorithm in many different areas of power system analysis such as system stability, coordination capacity… and has produced good results than other methods.

The purpose of this paper is to apply the improved particle swarm optimization algorithm to solve the optimal power flow problem with FACTS devices. Advanced IPSO method is tested and confirmed by comparing results with other methods such as Genetic Algorithm (GA), Simulated Annealing and Tabu Search (TS/SA), Evolutionary programming (EP).

2. FACTS MODELING FOR POWER FLOW STUDIES

2.1 Static VAR Compensator (SVC)

The simplest form of SVC consists of a TCR in parallel with a capacitor array as Figure 1. SVC is a variable reactance shunt connection, which is either generated or collected in reactive power to control voltage at the point of connection to the AC network [3]. It is widely used to provide fast reactive power for voltage regulation described in Figure 2. The stimulus angle control thyristor SVC allows almost instantaneous response.

Le Dinh Luong is with the Faculty of Mechanical - Electrical - Electronic, Ho Chi Minh City University of Technology (Hutech), Ho Chi Minh City, Viet Nam. E-mail: ledinhluong@gmail.com.

Dac Loc Ho is with Ho Chi Minh City University of Technology (Hutech), Ho Chi Minh City, Viet Nam. E-mail: hdloc@hcmhutech.edu.vn

Vo Ngoc Dieu (corresponding author) is with Ho Chi Minh City University of Technology, Ho Chi Minh City, Viet Nam. He is now with the Department of Power Systems. E-mail: vndieu@gmail.com.

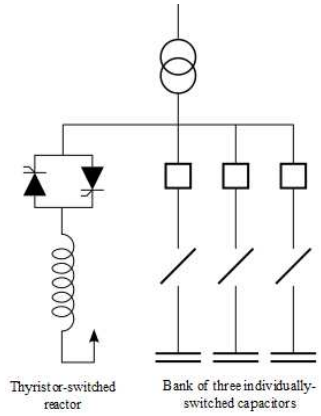

Fig. 1. Structural diagram of SVC.

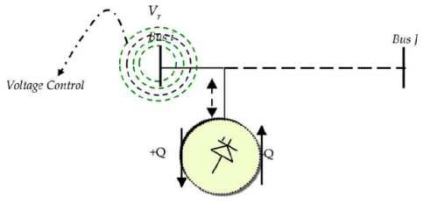

Fig. 2. Principle of voltage controlled shunt compensation devices FACTS.

Model of static compensators (SVC) is the VAr generator is presented Figure 3 that can pump or suction reactive power in the system is represented by Q_{SVC} [4].

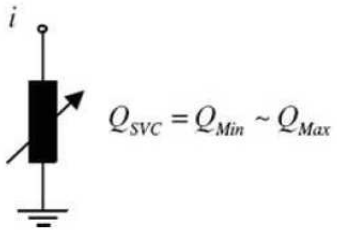

Figure 3. SVC model in power distribution [5].

2.2 Thyristor Controlled Series Capacitor (TCSC)

TCSC can change the electrical length of transmission lines. This feature enables the TCSC is used to quickly adjust power flow effects. It also increases the stability margin of the system and has proven very effective in reducing power oscillations [6]. Figure 4 describes the common structure of TCSC and Figure 5 describes the principles of the TCSC controller.

TCSC is integrated in the OPF problem by modifying the parameters of the road cord [7]. A new electric resistance (X_{new}) is as follows:

$$X_{new} = X_{ij} - X_C \quad (1)$$

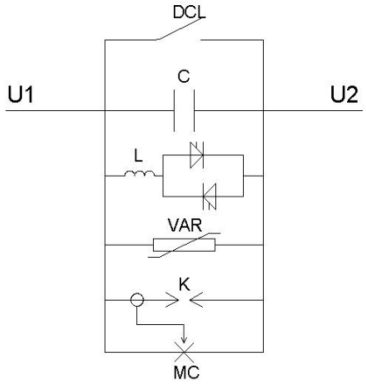

Fig. 4. Structural diagram of TCSC.

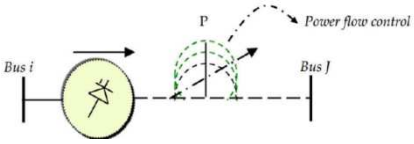

Fig. 5. The principle of power flow control serial devices FACTS.

3. OPF FORMULATION WITH FACTS DEVICES

In the OPF problem, the considered variables including control variables and state variables. The control variables include generating capacity of buttons except power balance, power pressure in the transmitter button, adjust the parameters of transformers and reactive power compensation capacitor rigs, FACTS parameters. The state variables include the transmit power of node balancing, load voltage, reactive power output of the generator, power flows on transmission lines. In addition, the OPF problem includes equality constraints are the power balance equations and inequalities bound the limits of the control variables and state variables. Generally, the OPF problem can be constructed as follows:

$$\text{Min } f(x,u) \quad (2)$$

subject to

$$g(x,u) = 0 \quad (3)$$

$$h(x,u) \leq 0 \quad (4)$$

where $f(x,u)$ is the objective function to be minimized, $g(x,u)$ is the set of equality constraints, and $h(x,u)$ is the set of inequality constraints.

x is the state variable vector, u is the control variable vector:

$$x = \left[P_{G_1}, Q_{G_1}, ..., Q_{G_{NG}}, V_{L_1}, ..., V_{L_{NL}} S_{l_1}, ..., S_{Nl}\right]^T \quad (5)$$

with no FACTS devices

$$u = \left[P_{G_2}, ..., P_{N_G}, V_{G_1}, ..., V_{G_{NG}}, Q_{C_1}, ..., Q_{cN_c} T_1, ..., T_{Nt}\right]^T \quad (6)$$

In case of FACTS devices, the control parameters of the device Q_{SVC}, Xc_{TCSC} be added to the control variables as follows:

$$u=\begin{bmatrix} P_{G_2},...,P_{N_G},V_{G_1},...,V_{G_{NG}},Q_{C_1},...,Q_{cN_c}T_1,...,T_{Nt}, \\ Q_1,..Q_{SVC},X_{C_1},...,X_{C_{NTCSC}} \end{bmatrix}^T \quad (7)$$

The fuel cost of each thermal generator is represented as a quadratic function of its power output.

$$MinF = \sum_{i=1}^{N} F_i(P_{Gi}) \quad (8)$$

F: total cost of the plant ($ / h).

$F_i(P_{Gi})$: fuel cost function of plant unit i ($ / h).

P_{Gi}: the capacity of plant unit i

N: total number of machines connected to the electrical system.

$$F_i(P_{Gi}) = a_i + b_i P_{Gi} + c_i P_{Gi}^2 \quad (9)$$

where a_i, b_i, c_i: Fuel cost coefficients of generating unit i

3.1 Real and Reactive Power Flow Equations

At each bus, the real and reactive power balance should be satisfied

a. Problem no FACTS

$$P_{Gi} - P_{di} = |V_i|\sum_{j=1}^{N_b}|V_j||Y_{ij}|\cos(\theta_{ij} - \delta_i + \delta_j); i = 1...N_b \quad (10)$$

$$Q_{Gi} + Q_{ci} - Q_{di} = |V_i|\sum_{j=1}^{N_b}|V_j||Y_{ij}|[\sin(\theta_{ij} - \delta_i + \delta_j)]; i = 1...N_b \quad (11)$$

P_{Gi}, Q_{Gi}: the active power, reactive injection at bus i.

P_{di}, Q_{di}: the active power, the reactive load.

Q_{ci}: the reactive power compensation of power at bus i.

$|V_i|, |V_j|$: is the voltage at bus i and bus j.

$|Y_{ij}|$: The value of component i, j of the resulting matrix.

ϕ_{ij}: is the phase angle of component i, j of the resulting matrix.

δ_i, δ_j: the voltage phase angle at bus i and j.

N_b: the total number of buses in the system.

b. Problem with FACTS

$$\begin{aligned} &P_{Gi} - P_{di} \\ &= |V_i|\sum_{j=1}^{N_b}|V_j||Y_{ij}(FACTS)|\cos(\theta_{ij}(FACTS) - \delta_i + \delta_j); \\ &i = 1...N_b \end{aligned} \quad (12)$$

$$\begin{aligned} &Q_{Gi} + Q_{ci} + Q_i(FACTS) - Q_{di} \\ &= |V_i|\sum_{j=1}^{N_b}|V_j||Y_{ij}(FACTS)|[\sin(\theta_{ij}(FACTS) - \delta_i + \delta_j)]; \\ &i = 1...N_b \end{aligned} \quad (13)$$

$Q_i(FACTS)$: the reactive power of FACTS devices at bus i.

$|Y_{ij}(FACTS)|$: the value of component i, j of matrix can lead mention FACTS devices.

3.2 Limits at Generation Buses

The real power, reactive power, and voltage at generation buses should be within between their lower and upper bounds.

$$P_{Gi,\min} \le P_{Gi} \le P_{Gi,\max}; i = 1...N_g \quad (14)$$

$$Q_{Gi,\min} \le Q_{Gi} \le Q_{Gi,\max}; i = 1...N_g \quad (15)$$

$$V_{Gi,\min} \le V_{Gi} \le V_{Gi,\max}; i = 1...N_g \quad (16)$$

N_g: Number of generators

3.3 Capacity Limits for Switchable Shunt Capacitor Banks

At var sources by switchable capacitors their power output should be within their lower and upper limits [5].

$$Q_{ci,\min} \le Q_{ci} \le Q_{ci,\max}; i = 1...N_c \quad (17)$$

N_c: number of sources to make the system.

3.4. Transformer Tap Settings Constraints

The tap settings of each transformer should be also within their lower and upper bounds.

$$T_{k,\min} \le T_k \le T_{k,\max}; k = 1...N_k \quad (18)$$

N_k: number of branches can adjust the voltage.

3.5 Security Constraints

The voltage at load buses and power flow in transmission lines should not exceed their limits.

$$V_{li,\min} \le V_{li} \le V_{li,\max}; i = 1...N_L \quad (19)$$

$$S_l \le S_{l,\max}; l = 1...N_l \quad (20)$$

N_l: number of line systems, N_L: number of nodes of the system load.

3.6 FACTS devices constraints

$$Q_{i,\min} \le Q_i \le Q_{i,\max}; i = 1...N_{SVC} \quad (21)$$

$$X_{ci,\min} \le X_{ci} \le X_{ci,\max}; i = 1...N_{TCSC} \quad (22)$$

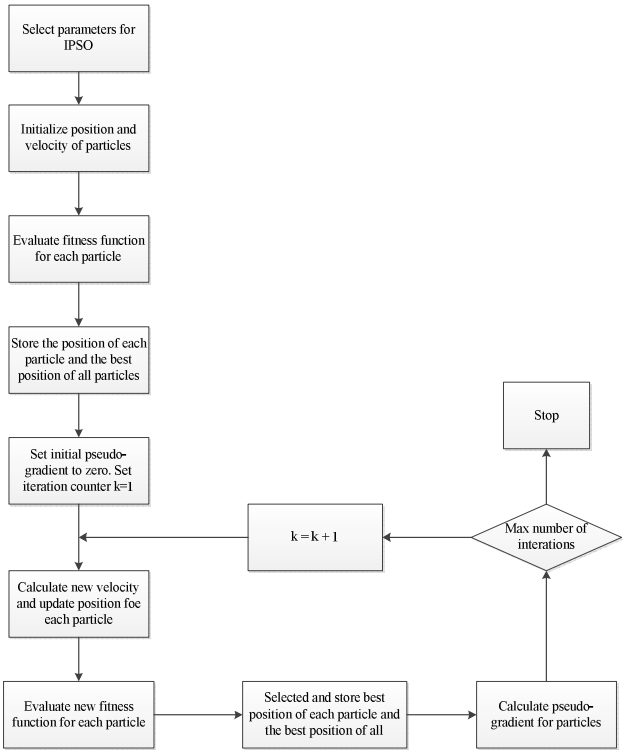

Fig. 6: Flowchart of IPSO for solving OPF problem.

4. 4. PARTICLE SWARM OPTIMIZATION

4.1. Conventional PSO

In PSO system, each individual adjusts its flying in a multi-dimensional search space according to its own flying experience and its companions flying experience. Each individual is referred to as a "particle" which represents a candidate solution to the problem. Each particle is treated as a point in a D-dimensional space [2]. The i[th] particle is represented as $Xi = (x_{i1}, x_{i2}, x_{i3},\ldots, x_{iD})$. The best previous position (giving the best fitness value) of any particle is recorded and represented as $P_I = (P_{i1}, P_{i2}, P_{i3},\ldots., P_{iD})$. The index of the best particle among all the particles in the population is represented by the symbol g. The rate of the position change (velocity) for particle i is represented as $V_i = (V_{i1}, V_{i2}, V_{i3},\ldots..,V_{iD})$. The particles are manipulated according to the following equation:

$$V_{id} = V_{id} + c_1 r_1 \left(P_{id} - X_{id}\right) + c_2 r_2 \left(P_{gd} - X_{id}\right) \quad (23)$$

$$X_{id} = X_{id} + V_{id} \quad (24)$$

where the constants c_1 and c_2 are cognitive and social parameters, respectively and r_1 and r_2 are the random values in [0, 1].

4.2. Improved Particle Swarm Optimization

The IPSO here is the PSO with constriction factor enhanced by the pseudo-gradient for speeding up its convergence process. The purpose of the pseudo-gradient is to guide the movement of particles in positive direction so that they can quickly move to the optimization. In the PSO with constriction factor [8,9], the velocity of particles is determined in (26) and (27).

In this case, the factor φ has an effect on the convergence characteristic of the system and must be greater than 4.0 to guarantee stability. However, as the value of φ increases, the constriction C decreases producing diversification which leads to slower response. The typical value of φ is (27) (i.e. $c_1 = c_2 = 2.05$).

$$V_{id} = C.\left[V_{id} + c_1 r_1 \left(P_{id} - X_{id}\right) + c_2 r_2 \left(P_{gd} - X_{id}\right)\right] \quad (25)$$

$$C = \frac{2}{\left|2 - \varphi - \sqrt{\varphi^2 - 4\varphi}\right|} \quad (26)$$

where $\varphi = c_1 + c_2, \varphi > 4$ (27)

The overall procedure of the proposed IPSO for solving the OPF problem is addressed in Figure 6.

Table 1. Result of OPF with TCSC

	No FACTS	TCSC
P_{g1} (MW)	177.9375	176.5955
P_{g2} (MW)	47.9981	47.6408
P_{g5} (MW)	21.0627	21.2075
P_{g8} (MW)	23.2693	24.0937
P_{g11} (MW)	10.0000	10.5641
P_{g13} (MW)	12.0000	12.0000
V_{g1} (pu)	1.1000	1.1000
V_{g2} (pu)	1.0844	1.0829
V_{g5} (pu)	1.0517	1.0550
V_{g8} (pu)	1.0653	1.0662
V_{g11} (pu)	1.1000	1.0839
V_{g13} (pu)	1.1000	1.1000
T_{11} (pu)	1.0000	1.0200
T_{12} (pu)	0.9100	0.9000
T_{15} (pu)	1.0300	1.0100
T_{36} (pu)	0.9500	0.9600
Q_{c10} (MVAr)	9.4000	0.0000
Q_{c24} (MVAr)	0.0000	4.3000
$TCSC_{3\text{-}4}$(pu)		0.0107
Ploss (MW)	8.8676	8.7016
Total cost ($/h)	799.9512	799.7741
Toltal Voltage deviation	1.3510	1.2481
Voltage stability index	0.1309	0.1319

5. NUMERICAL RESULTS

In this work the standard IEEE 30-bus test system has been used to test the effectiveness of the proposed method. It has a total of 8 control variables as follows:

six unit active power outputs, TCSC constraints and SVC constraints [11].

Three cases have been studied: Case 1 is the conventional OPF with TCSC devices using IPSO. Case 2 is the conventional OPF with SVC devices using IPSO. Case 3 is the conventional OPF with Multi FACTS devices using IPSO.

5.1. Optimal power flow with TCSC

In this case TCSC is considered in the OPF problem. The position of TCSC for this system according to [13] by loss sensitivity index indicates that branch 3-4 of system. In this simulation TCSC can change from 0 ~ 0.02 pu.

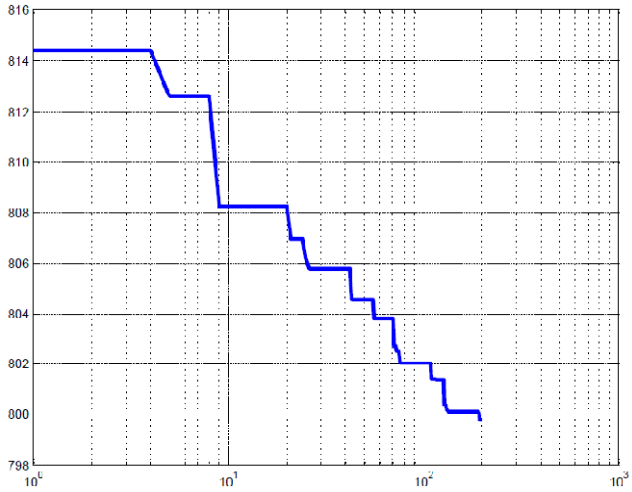

Fig. 7. Convergence characteristic of OPF with TCSC for the IEEE 30-bus system.

Table 2. Comparison of methods for OPF with TCSC

	TS/SA [12]	PSO [13]	IPSO
P_{g1} (MW)	192.6018	175.9641	176.5955
P_{g2} (MW)	48.4147	48.95	47.6408
P_{g5} (MW)	19.5561	21.526	21.2075
P_{g8} (MW)	11.6615	22.309	24.0937
P_{g11} (MW)	10	12.189	10.5641
P_{g13} (MW)	12	12	12.0000
$TCSC_{3-4}$ (pu)	0.02	0.011093	0.0107
Total cost ($/h)	804.6497	802.6552	799.7741

Results from Table 1 show that the TCSC is added to the system. Fuel costs for best solution is reduced from 799.9512 $/h in the absence of FACTS devices to 799.7741 $/h in the case with TCSC in line number 4 (line 3-4). As a result, the TCSC can lead to cost savings of 0.1771$/h or 0.022%. From the Table 2, we see IPSO can search for better solutions when compared with TS / SA [12], PSO in OPF problem with TCSC on IEEE30 bus system [13].

5.2. Optimal power flow with SVC

In this case, the SVC is considered in the OPF. SVC is placed at node 21 is the button with the reactive power demand in the highest load. SVC reactive power can be varied from 0 ~ 11.2 MVAr.

Table 3. Result of OPF with SVC

	No FACTS	SVC
P_{g1} (MW)	177.9375	177.2816
P_{g2} (MW)	47.9981	49.3202
P_{g5} (MW)	21.0627	19.5083
P_{g8} (MW)	23.2693	24.0881
P_{g11} (MW)	10.0000	10.0000
P_{g13} (MW)	12.0000	12.0000
V_{g1} (pu)	1.1000	1.1000
V_{g2} (pu)	1.0844	1.0863
V_{g5} (pu)	1.0517	1.0523
V_{g8} (pu)	1.0653	1.0565
V_{g11} (pu)	1.1000	1.1000
V_{g13} (pu)	1.1000	1.1000
T_{11} (pu)	1.0000	1.0900
T_{12} (pu)	0.9100	0.9000
T_{15} (pu)	1.0300	1.0100
T_{36} (pu)	0.9500	0.9700
Q_{c10} (MVAr)	9.4000	11.1000
Q_{c24} (MVAr)	0.0000	4.3000
SVC_{21} (MVAr)		8.2199
Ploss (MW)	8.8676	8.7982
Total cost ($/h)	799.9512	799.8193
Tolta voltage deviation	1.3510	1.2736
Voltage stability index	0.1309	0.1337

Table 4. Comparison of methods for OPF with SVC

	TS/SA [12]	PSO [13]	IPSO
P_{g1} (MW)	192.5895	176.1519	177.2816
P_{g2} (MW)	48.412	49.197	49.3202
P_{g5} (MW)	19.5554	21.533	19.5083
P_{g8} (MW)	11.6559	24.031	24.0881
P_{g11} (MW)	10	10	10.0000
P_{g13} (MW)	12	12	12.0000
SVC_{21} (MVAr)	11.196	6.4178	8.2199
Total cost ($/h)	804.5763	802.6454	799.8193

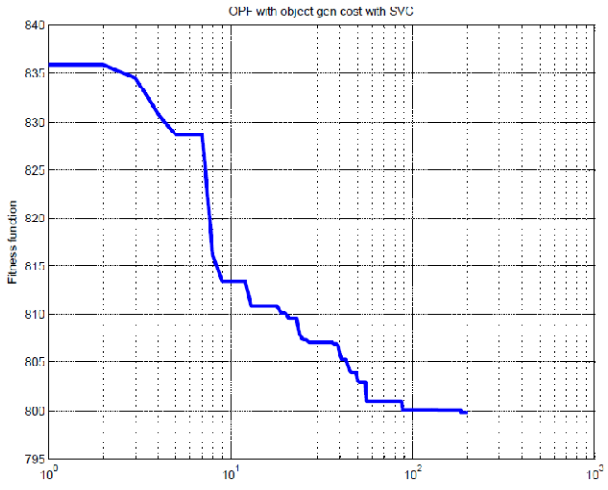

Fig. 8. Convergence characteristic of OPF with SVC for the IEEE 30-bus system

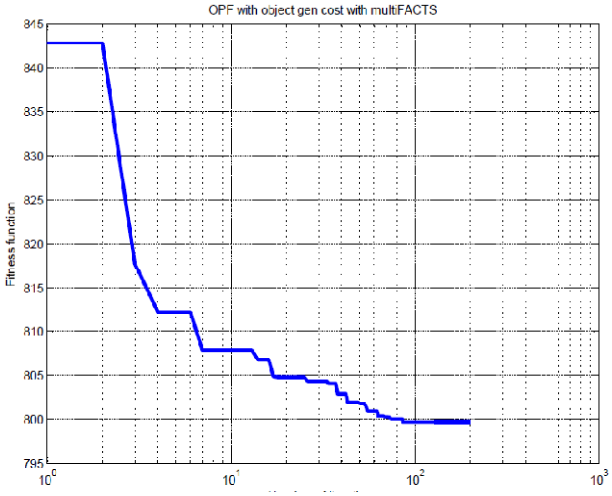

Fig. 9. Convergence characteristic of OPF with multi FACTS for the IEEE 30-bus system.

Table 5. Result of OPF with multi FACTS

	No FACTS	TCSC	SVC	Multi FACTS
P_{g1} (MW)	177.9375	176.5955	177.2816	178.8086
P_{g2} (MW)	47.9981	47.6408	49.3202	49.2240
P_{g5} (MW)	21.0627	21.2075	19.5083	21.7311
P_{g8} (MW)	23.2693	24.0937	24.0881	19.8779
P_{g11} (MW)	10.0000	10.5641	10.0000	10.6540
P_{g13} (MW)	12.0000	12.0000	12.0000	12.0000
V_{g1} (pu)	1.1000	1.1000	1.1000	1.1000
V_{g2} (pu)	1.0844	1.0829	1.0863	1.0873
V_{g5} (pu)	1.0517	1.0550	1.0523	1.0604
V_{g8} (pu)	1.0653	1.0662	1.0565	1.0693
V_{g11} (pu)	1.1000	1.0839	1.1000	1.1000
V_{g13} (pu)	1.1000	1.1000	1.1000	1.1000
T_{11} (pu)	1.0000	1.0200	1.0900	0.9700
T_{12} (pu)	0.9100	0.9000	0.9000	1.0000
T_{15} (pu)	1.0300	1.0100	1.0100	1.0000
T_{36} (pu)	0.9500	0.9600	0.9700	0.9800
Q_{c10} (MVAr)	9.4000	0.0000	11.1000	2.5000
Q_{c24} (MVAr)	0.0000	4.3000	4.3000	0.0000
SVC_{21} (MVAr)	-	-	8.2199	10.8107
TCSC (pu)	-	0.0107	-	0.0035
Ploss (MW)	8.8676	8.7016	8.7982	8.8956
Total cost ($/h)	799.9512	799.7741	799.8193	799.6030
Total voltage deiviation	1.3510	1.2481	1.2736	1.2989
Voltage stability index	0.1309	0.1319	0.1337	0.1344

Results from Table 3 show that the SVC was added to the system. Fuel costs for best solution is reduced from 799.9512 $/h in the absence of FACTS devices to 799.8193 $/h in the case of the SVC located at node 21. As a result, the SVC can lead to cost savings 0.1319 $/h or 0.017%. From the Table 4, we see IPSO can search for better solutions when compared with TS / SA, PSO in OPF with SVC problem on IEEE30 bus system.

5.3 Optimal power flow with multi FACTS

In this case TCSC and SVC are considered in the OPF problem. Table 5 shows the result of OPF with multi FACTS. Obviously, the total cost acquired by the multi Facts are all lower than that obtained by other case such as OPF with no Facts, OPF with TCSC and OPF with SVC.

6. CONCLUSION

In this paper, the improved particle swarm optimization (IPSO) algorithm has been presented to solve the optimal power flow problem considering FACTS devices. In the new improved method, the conventional IPSO algorithm is used with the variance coefficients to speed up the convergence to the global solution in a fast manner regardless of the shape of the cost function.

Calculation results show that the flexibility of PSO, IPSO in finding a global optimal solution that the other traditional algorithms can hardly be achieved. The algorithm can solve problems have complex objective function, not differentiable, have multiple discrete variables. Through comparison test shows IPSO algorithm has an advantage over PSO and TS/SA, so IPSO should be selected to solve the OPF problem with FACTS devices. A further direction for this study will be to apply other large-scale power systems with valve point effects and FACTS devices.

REFERENCES

[1] Kennedy, J. and Eberhart, R. C. 1995. Particle swarm optimization. In *Proceedings of IEEE*

International Conference on Neural Networks (ICNN'95), vol. IV, pp. 1942-1948, Perth, Australia.

[2] Jigar S. Sarda, Vibha N. Parmar, Dhaval G. Patel, "Lalit K.PatelGenetic Algorithm Approach for Optimal location of FACTS devices to improve system loadability and minimization of losses," *International Journal of Advanced Research in Electrical, Electronics and Instrumentation Engineering*, Vol. 1, Issue 3, September 2012.

[3] Mahdiyeh Eslami, Hussain Shareef, Azah Mohamed, and Mohammad Khajehzadeha 2012. Survey on Flexible AC Transmission Systems (FACTS). *Przegl Ąd Elektrotechniczny* (Electrical Review), vol. 88, pp. 1-11.

[4] Karthik, M. and Arul, M.P. 2013. Optimal Power Flow Control Using FACTS Devices. *International Journal of Emerging Science and Engineering* vol. 1, no. 12, pp. 1-4.

[5] Madhusudhana Rao, G., Sanker Ram, B.V. and Sampath Kumar, B. 2010. TCSC designed optimal power flow using genetic algorithm. *International Journal of Engineering Science and Technology*, vol. 2, no. 9, pp. 4342-4349.

[6] Thanushkodi, K., Muthu Vijaya Pandian, S., Dhivy Apragash, R.S., Jothikumar, M., Sriramnivas, S. and Vindoh, K. 2008. An efficient particle swarm optimization for economic dispatch problems with non-smooth cost functions. *WSEAS Transactions on Power Systems*, vol. 3, no. 3, pp. 257-266.

[7] Yuhui Shi and Russell Eberhart 1998. A Modified Particle Swarm Optimizer. In *Proceedings of IEEE International Conference on Evolutionary Computation*, Anchorage, 4-9 May, p. 69 – 73.

[8] Russell C. Eberhart and Yuhui Shi 2001. Particle Swarm Optimization: Developments, Applications and Resources. In *Proceedings of the 2001 Congress on IEEE Evolutionary Computation*, vol. 1, p 81 - 86.

[9] Pandian Vasant. 2013. Meta-HeuristicsOptimization Algorithmsin Engineering, Business, Economics, and Finance. IGI Global Publisher.

[10] Zimmerman, R. D., Murillo-Sánchez, C. E. and Thomas, R. J. 2011. MATPOWER Steady-State Operations, Planning and Analysis Tools for Power Systems Research and Education. *IEEE Transactions on Power Systems*, vol. 26, no. 1, pp. 12-19.

[11] Ongsakul, W. and Bhasaputra, P. 2002. Optimal Power Flow with FACTSDevices by Hybrid TS/SA Approach. *International Journal of Electrical Powerand Energy Systems*, vol. 24, pp. 851-857.

[12] Nuttachai Puttanon. 2007. Optimal power flow with facts devices by particle swarm optimization. *M.Eng. Thesis*, Unpublished, AIT, Thailand.

Application of Cuckoo Search Algorithm for Optimal Power Flow in Power System

Le Anh Dung and Vo Ngoc Dieu

Abstract*— *The cuckoo search algorithm is applied in many scientific fields such as computer, mechanic and power system. Especially, the cuckoo search can solve and give results in optimization problems with many variables and constraints. A advance of cuckoo search algorithm is solving time which can solve the problems with short time and many iterations. This paper research and apply the algorithm for optimization power flow in power system operation. The research also tests this algorithm by IEEE 30 bus system and use Matlab software to launch optimization program. The results of progress show that the cuckoo search algorithm has many advantages more than former particle swarm optimization methods.

***Keywords*— Cuckoo search algorithm, particle swarm optimization, optimal power flow.**

1. INTRODUCTION

Power flow optimization is important problem in power system operation. Especial, it become difficult and complicated when power system has many power plants, many loads, transmission substations, transformer tap changers and more capacitors. The main target of optimal power flow problem is power on transmission lines, capacity of capacitor banks, and tap changer level with minimum cost of generation in system.

There are many methods to solve optimal problem, classical methods are Lagrange algorithm and Newton method, artificial intelligence methods such as GA (Genetic Algorithm), DE (Differential Evolution), Particle swarm optimization (PSO) and PSO improvement [1][2][3]. Artificial intelligence methods have some advantages more than classical methods, it can solve optimal problem with quadratic functions and sum functions which are available in fuel function of thermal generation in power system. From 2004, PSO and PSO improvement methods such as PSO with Time-Varying Acceleration Coefficients (PSO-TVAC), Pseudo Gradient PSO (PG-PSO), Pseudo Gradient PSO Constriction Factor (PG-PSOCF) [4][5][6] were researched for economic dispatch optimal operation in power system.

Cuckoo Search Algorithm (CAS) is new algorithm in optimization field nearly years. Furthermore, CS combine Levy flights were used in information technology and other science technical fields from 2009 up today [7][8][9][10][11][12]. However, there are very little CS application for optimal power flow (OPF) in power system operation.

This paper introduces new method to solve OPF problem which is CS algorithm. CSA can be method bester than classical methods or PSO and PSO improvement because CS method has quick convergence, so CS method can save time and give good results. From these advantages, so CSA can be applied in large scale power system with many constraints and other requirements of power system operation.

In this paper, Section 2 shows OPF formulas and constraints equations in power system operation. Section 3 build CSA and Lévy flights distribution. Section 4 applies CAS for OPF problem. Section 5 gives results of OPF problem with data IEEE 30 bus system which are solved by CSA. The results also compare to some previous methods the same OPF problem.

2. PROBLEM FORMULATION

Target of OPF problem in powers system operation is voltage, current, power load, reactive power and capacitor values of each bus in system with minimum generator cost [13][14][15][16]. In addition, OPF problem is very important because it should calculate about balance power between generators and load demands, quality of voltage, current and power which supply to customers.

Objective function

The objective function of OPF problem is:

$$MinF = \sum_{i=1}^{N_g} F_i(P_{gi}) \quad (1)$$

Cost function of thermal generators is:

$$\text{Min } F = \sum_{i=1}^{NG} \left(a_i + b_i P_{Gi} + c_i P_{Gi}^2 \right) \quad (2)$$

Cost function of thermal generator with vale point effect:

Le Anh Dung is with Binh Duong Power Company, South Power Company, Electricity of Vietnam. He is now doctoral student at Ho Chi Minh City University of Technology, Ho Chi Minh City, Vietnam. E-mail: dungle444@yahoo.com.

Vo Ngoc Dieu (corresponding author) is with Ho Chi Minh City University of Technology, Ho Chi Minh City, Vietnam. He is now with the Department of Power Systems. E-mail: vndieu@gmail.com.

$$\text{Min } F = \sum_{i=1}^{N_g} \left(\begin{array}{l} a_i + b_i P_{gi} + c_i P_{gi}^2 + \\ \left| e_i \sin(f_i (P_{gi,\min} - P_{gi})) \right| \end{array} \right) \quad (3)$$

Constraint factors

Balance of power and reactive power

$$P_{gi} - P_{di} = V_i \sum_{j=1}^{N_b} V_j \left[G_{ij} \cos(\delta_i - \delta_j) + B_{ij} \sin(\delta_i - \delta_j) \right] \quad (4)$$

$i = 1, ..., N_i$

$$Q_{gi} + Q_{ci} - Q_{di} = V_i \sum_{j=1}^{N_b} V_j \left[\begin{array}{l} G_{ij} \sin(\delta_i - \delta_j) + \\ B_{ij} \cos(\delta_i - \delta_j) \end{array} \right] \quad (5)$$

$i = 1, ..., N_i$

Limit of power and reactive power each generator bus

$$P_{gi,\min} \le P_{gi} \le P_{gi,\max}; \;\; i = 1, ..., N_g \quad (6)$$

$$Q_{gi,\min} \le Q_{gi} \le Q_{gi,\max}; \;\; i = 1, ..., N_g \quad (7)$$

$$V_{gi,\min} \le V_{gi} \le V_{gi,\max}; \;\; i = 1, ..., N_g \quad (8)$$

Transformer tap setting constraints

$$T_{k,\min} \le T_k \le T_{k,\max}; \;\; k = 1, ..., N_i \quad (9)$$

Voltage and power flow constrains at load buses and transmission line

$$V_{li,\min} \le V_{li} \le V_{li,\max}; \;\; i = 1, ..., N_d \quad (10)$$

$$S_l \le S_{l,\max}; \;\; i = 1, ..., N_i \quad (11)$$

3. CUCKOO SEARCH ALGORITHM

Cuckoo search algorithm (CSA) is a new meta-heuristic algorithm inspired from the nature for solving optimal problems. The basic idea of this algorithm is based on the obligate brood parasitic behavior of some cuckoo species in combination with the Lévy flight behavior of some birds and fruit flies. In nature, cuckoo birds usually lay their eggs in nests of the other bird species (host nests). There are some cases which can happen. First, the birds of host nests know the eggs of cuckoo birds (alien eggs) and they can reject it throw out their nests or they release their nests and build new nests. Second, the birds of host nests do not know alien eggs and it will become cuckoo birds. Following cuckoo behavior, CSA described as three main steps [17]

- Each cuckoo lays one egg (a design solution) at a time and dumps its egg in a randomly chosen nest among the fixed number of available host nests;
- The best nests with high a quality of egg (better solution) will be carried over to the next generation;
- A host bird can discover an alien egg in its nest with a probability of $p_a \in [0, 1]$. In this case, it can simply either throw the egg away or abandon the nest and find a new location to build a completely new one.

The Lévy flight distribution

In nature, animals can search for food in a random or quasi-random manner. Generally, the foraging path of an animal is effectively a random walk since the next move is based on the current location state and the transition probability to the next location. The chosen direction depends implicitly on a probability which can be mathematically modeled. Recent various studies have shown that the flight behavior of many animals and insects has demonstrated the typical characteristics of Lévy flights following step [18]:

$$Lévy \sim u = t^{-\lambda}, (1 < \lambda \le 3) \quad (12)$$

4. CSA APPLICATION FOR OPF PROBLEM

Fitness function of OPF problem is:

$$F_{fitness} = F(x,u) + K_P \sum_{i=1}^{N_g} \left(P_{gi} - P_{gi}^{\lim} \right)^2 + K_q \sum_{i=1}^{N_g} (Q_{gi} - Q_{gi}^{\lim})^2 + K_v \sum_{i=1}^{N_d} (V_{li} - V_{li}^{\lim})^2 + K_s \sum_{l=1}^{N_l} (S_l - S_{l\max})^2 \quad (13)$$

Overall procedure of CSA for OPF problem following as steps:

Step 1: Choose bird nests N_p, parameters of CSA: p_a, IT_{max}, total generators N includes cost function parameters a_i, b_i, c_i, e_i, f_i. Power of generators P_{gi} correspond number of cuckoo eggs in nest N.

Step 2: Slack power P_s calculation and choose initial output power of generators. Use Matpower 4.1 Toolbox to calculate:

- Value objective function FC.
- Reactive power of generators Q_g.
- Bus voltage of generators V_g, and voltage of load bus V_l.
- Power on transmission lines S_l.
- Voltage output of tap changer V_T, capacity of capacitors Q_C.
- Value of fitness function FF_{inf}.

Step 3: Apply Lévy flights distribution to choose the eggs of cuckoo corresponding with initial power output of generators. Calculate FC, Q_g, V_g, V_{load}, S_l, V_T, Q_c. From these results, calculate new value of fitness function FF_{new}.

Step 4: Assess quality of initialized cuckoo eggs.

– If $FF_{new} > FF_{inf}$ reject initialized eggs.

– If $FF_{new} < FF_{inf}$ continue to run iterations and reject number of eggs with p_a probability.

Step 5: From p_a rejected eggs, calculate fitness function FF_{dis}.

Step 6: Continue program to maximum iteration IT_{max}, compare and assess value of FF_{new} and FF_{dis}, choose the eggs with the best quality corresponding power output of generators with minimum cost FF.

Step 7: Diagram characteristic of FF with each iteration.

Step 8: Show result of problem: P_{gi}, FC, P_{loss}, Q_g, V_g, V_{load}, S_l, V_T, Q_c, iterations, programming time of computer.

5. NUMERICAL RESULTS

The CSA for OPF problem is tested on IEEE 30 bus system. Target of problem is minimum operation cost with the best parameters about voltage at generator and load buses, power output of generators, power loss, power on transmission lines, reactive power of generators, capacity of capacitors, and voltage of tap changers. The data of IEEE 30 bus give on Table 1

Table 1. IEEE 30 bus system data

IEEE 30 buses	Total	Bus No.
Generators	6	1, 2, 5, 8, 11, 13
Transformers	4	6-9, 6-10, 4-12, 27-28
Capacitor banks	9	10, 12, 15, 17, 20, 21, 23, 24, 29
Tap changers	4	4, 6, 10, 28
Branches	41	From 1 to 30
Loads	24	3, 4, 6, 7, 9, 10, 12, 14 to 30

The program has been developed in Matlab software and Power Toolbox 4.1 [19] to solve OPF problem with CSA. The parameters of the CSA are selected as follows: the number of nest N_p = 15, probability for an alien egg to be discovered p_a = 0.25, maximum number of iterations It_{max} = 100, penalty factor for fitness function $K = 10^6$. For obtaining the optimal solution, the algorithm is performed 20 independent runs.

The results of CSA for OPF problem show on figures and tables, appendixes. Table 2 shows voltage of tap changers, table 3 give results of capacitor banks, table 4 shows power, reactive power and voltage of generators, table 5 compare efficient between CS and different artificial intelligence methods. Appendix 1 is voltage results of load buses. Appendix 2 shows power flow on transmission lines.

The final results were compared with other methods such as DE, Weight Inertia-PSO (WIPSO), GA, Sequential Quadratic Programming (SQP), Simulated Annealing (SA), Newton-based Optimal Power Flow (NOFP), Extended Dommel-Tinny OPF (ED-OPF), and Improved Evolutionary Programming (IEP) [20][21][22].

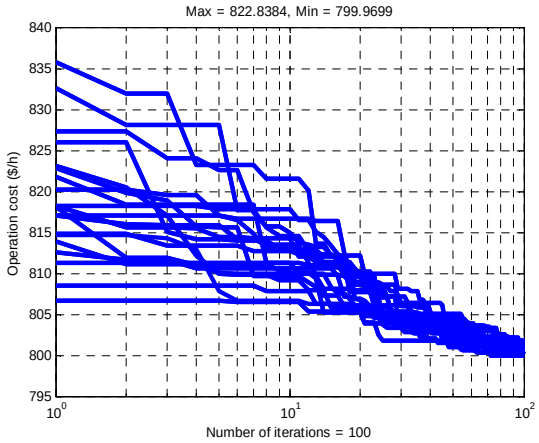

Fig. 1. The convergence characteristics of CSA for cost OPF problem with 20 running.

Table 2. Voltage at Tap changer buses

Bus No.	4	6	10	28
V_T (p.u)	1.07	0.98	1.10	1.02

Table 3. Capacity of capacitor banks

Bus No.	10	12	15	17	20
Q_c	4.65	2.20	0.77	0.00	5.00
Bus No.	21	23	24	29	
Q_c	5.00	5.00	0.66	0.82	

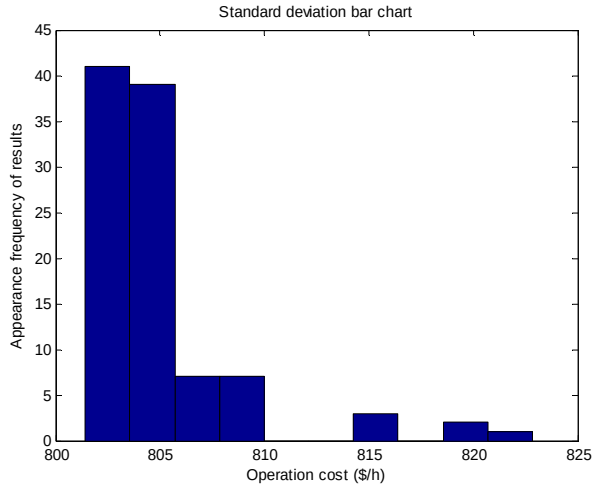

Fig. 2. The statistic chart of CSA for cost of OPF problem after 20 running.

Table 4. Power and voltage generator buses resultes

Bus No.	Power generation P_{gi} (MW)	Voltage generator buses V_{gi} (p.u)	Reactive power generation Q_{gi} (MVAr)
1	174,4256	1.10	-7.27
2	47,8077	1.08	6.33
5	19,5673	1.05	20.99
8	23,9503	1.06	18.12
11	10,0000	1.07	22.01
13	16,4716	1.10	44.57

Table 5. Compareation of the best results between methods

Method	Min. cost ($/h)	Standard deviation	IT_{max}	Time running (s)
DE [20]	801,23	-	100	30,945
WI-PSO [21]	799,1665	-	200	15,4
GA [21]	801,24	-	-	-
SQP [21]	802,23	-	200	20
SA [22]	803,97	2.6317	150	28,29
NOFP [22]	805.45	-	-	-
EDOPF [22]	813,74	-	-	-
IEP [22]	802,58	-	-	99,013
PSO TVAC	798,9687	0,3640	100	8,84
PG PSO	799,5107	1,9276	100	4,59
PG PSO CF	798,9997	2,5343	100	4,48
CS	**799,9699**	**0,5493**	**100**	**8,97**

6. CONCLUSION

Although particle swarm optimization algorithms such as PSO, DE, GA have advances in optimal power system operation. However, CS algorithm is new method and has fortes more than former methods. In OPF problem, CS algorithm can solve and give accurate results with short progress CPU time. CSA also has quick convergence after some iterations.

The results on table 5 and appendix 1, 2 show effecient of CS method which can solve more complicated or bigger problems in power system. Especialy, when renewable energy become popular in power generation, OPF problem calculation need exact and fast progress. The CS algorithm is new method which can help to solve OPF problem in future.

NOMENCLATURE

N_p	Number of particles.
P_D	Total system load demand.
a_i,b_i,c_i	Cost coefficients for quadratic cost function of generator *i*.
e_i, f_i	Cost coefficients of generator *i* reflecting valve-point effects.
B_{ij}, B_{0i}, B_{00}	B-matrix coefficients for transmission power loss.
N_g	Number of generators.
P_{gi}	Power output of generator *i*.
$P_{gi,min}$, $P_{gi,max}$	Minimum and maximum power outputs of generator *i*, respectively.
Q_{gi}	Reactive power output of generator *i*.
$Q_{gi,min}$, $Q_{gi,max}$	Minimum and maximum reactive power outputs of generator *i*.
P_L	Total transmission loss.
V_{gi}	Voltage of generator *i*.
V_{li}	Voltage of line number *i*.
S_{li}	Power on transmission line *i*.
T_k	Tap changer level position.
FF_{inf}	Initial value of fitness function.
FF_{new}	Value of fitness function applied Lévy flights distribution.
FF_{dis}	Value of fitness function calculated from reject eggs with p_a probability.

REFERENCES

[1] Kennedy, J. and Eberhart, R. 1995. Particle swarm optimization. In *Proc. IEEE Conf. Neural Networks* (ICNN'95), Perth, Australia, 1995, vol. IV, p. 1942–1948.

[2] Mahor, A., Prasad, V. and Rangnekar, S. 2009. Economic dispatch using particle swarm optimization: A review. *Renewable and Sustainable Energy Reviews*, vol. 13, no. 8, pp. 2134-2141.

[3] Ratnaweera, A., Halgamuge, S. K. and Watson, H. C. 2004. Self-organizing hierarchical particle swarm optimizer with time-varying acceleration coefficients. *IEEE Trans. Power Systems*, vol. 8, no. 3, pp. 240-255.

[4] Pham, D.T. and Jin, G. 1995. Genetic algorithm using gradient-like reproduction operator. *Electronic Letter*, vol. 22, no.18, pp. 1558-1559.

[5] Zhou Wu, Tommy W. S. Chow 2012. A local multiobjective optimization algorithmusing neighborhood field. Department of Electronic Engineering, City University of Hong Kong, Kowloon, Hong Kong.

[6] Lee, T.-Y. 2008. Short term hydroelectric power system scheduling with wind turbine generators using the multi-pass iteration particle swarm optimization approach. *Energy Conversion and Management*, vol. 49, pp. 751–760.

[7] Clerc, M. & Kennedy, J. (2002). The particle swarm - Explosion, stability, and convergence in a multidimensional complex space. *IEEE Trans. Evolutionary Computation*, vol. 6, no. 1, pp. 58-73.

[8] Pandian Vasant 2013. Meta-Heuristics Optimization Algorithm in Engineering, Business, Economics, and Finance, IGI Global, pp. 1-37.

[9] Yang, X.-S., Deb, S. 2009. Cuckoo search via Lévy flights. In *Proc. World Congress on Nature &*

Biologically Inspired Computing (NaBIC 2009), India, 2009, pp. 210-214.

[10] Yang, X.-S. and Deb, S. 2010. Engineering optimisation by cuckoo search. *Int. J. Mathematical Modelling and Numerical Optimisation*, vol. 1, no. 4, pp. 330-343.

[11] Dieu, V.N., Schegner, P., and Ongsakul, W. 2011. A newly improved particle swarm optimization for economic dispatch with vanve point loading effects. In *Proc. IEEE Power & Energy Society General Meeting*, USA, July 2011.

[12] Brini, S., Abdallah, H. H. and Ouali, A. 2009. Economic dispatch for power system included wind and solar thermal energy. Leonardo Journal of Sciences, no. 14, pp. 204-220.

[13] Liang, R.-H. and Liao, J.-H. 2007. A fuzzy-optimization approach for generation scheduling with wind and solar energy systems. IEEE Trans. Power Systems, vol. 22, no. 4, pp. 1665-1674.

[14] Shi, L. B., Wang, C., Yao, L. Z., Wang, L. M., Ni, Y. X. and Masoud, B. 2010. Optimal power flow with consideration of wind generation cost. *Int. Conference on Power System Technology* (POWERCON), 24-28 Oct., Hangzhou, China.

[15] Chen, G., Chen, J. and Duan, X. 2009. Power flow and dynamic optimal power flow including wind farms. *Int. Conference on Sustainable Power Generation and Supply*, SUPERGEN '09, 6-7 April, Nanjing, China.

[16] Jabr, R.A. and Pal, B.C. 2009. Intermittent wind generation in optimal power flow dispatching. *IET Generation, Transmission & Distribution*, vol. 3, no. 1, pp. 66-74.

[17] Dieu, V.N., Schegner, P., and Ongsakul, W. 2013. Cuckoo search algorithm for nonconvex economic dispatch", IET Generation, transmission and distribution, vol. 7, no. 6, pp. 645 – 654.

[18] Sangita, R. and Sheli, S. 2013. Cuckoo search algorithm using Lévy flight: a review. *I. J Modern Education and Computer Science*, Published Online December 2013, in MECS, p10-15.

[19] Zimmerman, R. D., Murillo-Sánchez, C, E, and Thomas, R. J. 2010. MATPOWER Steady-State Operations, Planning and Analysis Tools for Power Systems Research and Education. *IEEE Transactions on Power Systems*, vol. 26, no.1, pp. 12-19.

[20] Mahor, A., Prasad, V. and Rangnekar, S. 2009. Economic dispatch using particle swarm optimization: A review. *Renewable and Sustainable Energy Reviews*, vol. 13, pp. 2134-2141.

[21] Suharto, M. N., Hassan, M. Y., Majid, M. S., Abdultah, M. P., and Hussin, F. 2011. Optimal power flow solution using evolutionary computation techniques. *IEEE Region 10 Conference*, p. 113 – 117.

[22] Sousa, T., Pinto, I., Morais, H., and Vale, Z. 2012. Simulated Annealing meta-heuristic to solve the optimal power flow. *3rd IEEE PES International Conference and Exhibition on Innovative Smart Grid Technologies (ISGT Europe)*, p. 1 - 8.

APPENDIX

Table A1. Load buses voltage result

Bus	V_{max}	V_{min}	V
3	1.06	0.94	1.07
4	1.06	0.94	1.07
6	1.06	0.94	1.06
7	1.06	0.94	1.06
9	1.06	0.94	1.09
10	1.06	0.94	1.08
12	1.06	0.94	1.05
14	1.06	0.94	1.04
15	1.06	0.94	1.04
16	1.06	0.94	1.05
17	1.06	0.94	1.07
18	1.06	0.94	1.05
19	1.06	0.94	1.04
20	1.06	0.94	1.04
21	1.06	0.94	1.02
22	1.06	0.94	1.00
23	1.06	0.94	1.02
24	1.06	0.94	1.06
25	1.06	0.94	1.00
26	1.06	0.94	0.99
27	1.06	0.94	1.04
28	1.06	0.94	1.04
29	1.06	0.94	1.02
30	1.06	0.94	1.00

Table A2. Transmision lines power result

Bus	From bus	To bus	S_{max} (MVA)	S_l
1	1	2	130	114.67
2	1	3	130	63.61
3	2	4	65	34.79
4	3	4	130	59.85
5	2	5	130	62.56
6	2	6	65	46.28
7	4	6	90	55.58
8	5	7	70	11.29
9	6	7	130	33.62
10	6	8	32	20.27
11	6	9	65	25.91
12	6	10	32	16.90
13	9	11	65	26.45
14	9	10	65	31.85
15	4	12	65	41.62
16	12	13	65	46.15
17	12	14	32	7.73
18	12	15	32	17.71
19	12	16	16	7.41
20	14	15	16	1.31
21	16	17	16	3.39
22	15	18	16	5.57
23	18	19	16	2.28
24	19	20	16	8.08
25	10	20	32	9.56

26	10	17	32	7.37
27	10	21	32	17.17
28	10	22	32	8.27
29	21	22	32	1.51
30	15	23	16	4.78
31	22	24	16	6.71
32	23	24	16	4.27
33	24	25	16	0.99
34	25	26	16	4.26
35	25	27	16	5.04
36	28	27	65	18.79
37	27	29	16	6.28
38	27	30	16	7.23
39	29	30	26	3.80
40	8	28	32	3.30
41	6	28	32	17.23

Renewable Energy for Rural Electrification in Thailand: A Case Study of Solar PV Rooftop Project

Wichit Krueasuk, Pornrapeepat Bhasaputra, Woraratana Pattaraprakorn, and Supattana Nirukkanaporn

Abstract*— *Rural electrification (RE) is still remained to be a challenge for Thailand due to its sparse electricity demand in the remote areas. Expansion of the electricity transmission and distribution service to such area is difficult and uneconomic. The use of renewable energy technologies not only offers an environmental friendly and economically viable for RE, but also aligns with the National Agenda to promote the use of renewable as alternative energy resources to reduce the dependency of imported fuel and increase fuel diversification. The Thai government is targeting 25% of the energy generation from renewable energy resources by the year 2021. The government has established and implemented several projects to promote the use of renewable energy, especially solar PV systems. This paper proposes an analysis of the problems encountered during the progress of this RE program, with the use of data obtained from Provincial Electricity Authority (PEA). The analysis takes into account of the uncertainty of PV generation and investment conditions. Under economic analysis, the levelized cost of electricity (LCOE) method is used to evaluate the designed system with a comprehensive way to find the LCOE optimized of RE in Thailand. The results provide a positive support to government investment in subsidy program for the implementation of solar PV system for RE.

***Keywords*— Rural Electrification, Renewable Energy, PV, LCOE.**

1. INTRODUCTION

The Eleventh National Economic and Social Development Plan (NESDP: 2012-2016) of Thailand [1] has main objectives to reduce poverty and tackle inequality. Its timeline is shown in Fig.1. The infrastructure is solution for the development benefits of solving the problem of structural injustice. The NESDP targeted establish to reduce the income gap of the population and reduce inequality in access to the basic social services and the economic opportunities. It also aims to provide sufficient infrastructure as well as electrical system to cover the populated areas of the country. In particular, rural electrification is a service to raise the quality of life, income distribution and economic diversification in disperse areas.

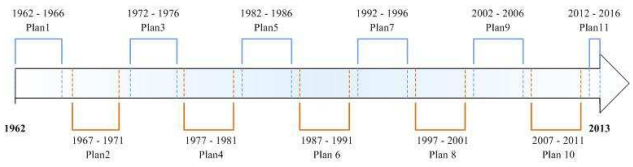

Fig.1. Timeline of NESDP

The Fifth NESDP in 1982-1986, emphasized the development of the efficiency power supply and the energy conservation, consequently the government have policy for subsidy the energy source from renewable energy. The NESD planning has the preparation to support the renewable energy in a sustainable way to reduce pollution and the energy imports.

Electricity supply development is considered to be an in economic investment in the remote areas or the scattered demand areas for the utility supply industries. In the past, RE have utilized diesel generators to supply electricity the consumption of diesel oil as fuel has resulted in expensive generation cost, which brought the per unit generation cost of electricity in remote areas. Therefore, renewable energy such as solar power, wind power and hydro-power provides solution for RE system in Thailand.

Incessantly, the renewable energy is supported by Thai government accord the Power Development Plan 2010-2030 Rev.3: PDP2010 [2] and Renewable Energy Development Plan: REDP2008-2022[3]. REDP have targeting development of renew energy for about 12 % in 10 years, the new Renewable and Alternative Energy Development Plan: AEDP 2012-2021[4] is aiming for an incremental of 25 % in 15 years. The power generation from renewable energy technologies is promoted by the "Adder" and "Feed-in Tariff (FIT)" measures. Presently, the Solar PV Rooftop is emphatic for the power generation from the solar PV with total capacity purchase is 200 MW. The government subsidy for the project is the FIT for the medium-large and factory businesses, the small businesses and household in the rate are 6.96 Baht/kWh, 6.55 Baht/kWh and 6.16 Baht/kWh respectively for 25 years [5]. The population near the grid benefits both from the subsidy and system stability while the rural area population does not. The promotion government has created social inequality with regard to the accessibility to electricity and benefits from renewable energy subsidized program; hence,

Wichit Krueasuk (corresponding author) and P. Bhasaputra are with Department of Electrical Engineering, Faculty of Engineering, Thammasat University, 99 M18 Phaholyothin Road, Khlongluang, Pathumthani, 12120, Thailand. E-mail: wichit.kr@spu.ac.th, bporr@engr.tu.ac.th.

W. Pattaraprakorn is with Department of Chemical Engineering, Faculty of Engineering, Thammasat University, 99 M18 Phaholyothin Road, Khlongluang, Pathumthani, 12120, Thailand. E-mail: pworarat@engr.tu.ac.th.

opportunities in the management of solar PV system for RE should be provided for rural population.

The appropriate time for investments of solar PV is presented by LCOE method, considering different scenario for PV sizes, sun hour and discount rate. The analysis incorporates various parameters corresponding to economic investment and the society solution for RE. The paper is structured as follows. Section 2 presents conceptual background about the rural electrification, renewable energy and solar PV project in Thailand. Section 3 defines the analytical model of LCOE of a technology as the sum of generation costs and integration costs per generation unit of that technology. Section 4 expands the solution method, followed by results and discussion in section 5. Section 6 summarizes and concludes.

2. BACKGROUND

2.1 Rural Electrification in Thailand

Electrification vated vary significantly across countries in the Asia and the Pacific (Table 1) . Typically, South and Southeast Asian countries are characterized by high and high density populations with about 59.2% and 37.8%, respectively, of their total populations not yet having access to electricity [6].

Table 1 Electrification access rate in Asia and the Pacific

Region					
South Asia		Southeast Asia		East Asia Pacific	
Country	%	Country	%	Country	%
Sri Lanka	62	Singapore	100	Marshal Island	100
Pakistan	52.9	Thailand	98.5	China	98.6
India	43	Malaysia	96.9	Tonga	85
Bangladesh	32.5	Philippines	87.4	Fiji	80
Nepal	15.4	Vietnam	75.8	Palau	60
		Indonesia	53.4	Papua New Guinea	46
		Cambodia	15.8	Micronesia	45
		Myanmar	5	Kiribath	40
		Laos	NA	Vanuatu	26
				Timor-Leste	22
				Solomon Islands	15

Low power energy consumption of the household Thai villages in rural area, especially the electric energy consumption. Most people in rural are poor and the cooking consume the wood gathered from the surroundings for charcoal production, the kerosene wick lamps and candles are used for lighting at night. They need electricity for just in case very basic essential needs such as use TV and radio and using electricity for just a few hours at night. Usually, the households have 4 to 5 people with 5 to 10 houses of small villages and 50 to 100 houses of large village in Thai villages rural. Moreover, many villages are difficult to the travel enter the distance about 5 km to 40 km, especially in mountainous regions or the island.

The rural electrification (RE) program in Thailand was implemented through Provincial Electricity Authority (PEA), which is responsible for electricity distribution in provinces as Provincial Electricity Organization (PEO) was established in 1954. PEO is the responsibility to generate and distribute electricity to all areas in Thailand except the Bangkok metropolitan areas, it was renamed PEA in 1960. The Metropolitan Electricity Authority (MEA) was responsible for distribution in the Bangkok Metropolitan Area. In 1969 the Electricity Generating Authority of Thailand (EGAT) was established, EGAT consolidate different organizations that generating electricity to meet the growing electricity demand, with mandate for generation and transmission system. EGAT, PEA and MEA are state enterprises with responsibilities were limited to the distribution of electricity in their respective jurisdictions. In 1992, Independent power producers (IPPs) were allowed to generate electricity sell to EGAT. EGAT continues to be the sole agency responsible for transmission.

PEA initiate the rural electrification program in 1977 based on the 25-year “National Plan for Accelerated Rural Electrification"[7]. The long-term plan was divided into 5- year plans to relate the 5-year national economic and social development plans (NESDP) of the country. Each plan set specific targets for increasing electricity access in rural areas[8]. Office of Rural Electrification (ORE) was established by PEA for planning and implementing the RE programmer. In Thailand, rural electrification efforts during the 1960s were through use of decentralized diesel-generating plants. The growth of electrification was relatively low during this period and only 7% of the rural households had access to electricity in early 1970s. In 1978, a year after initiation of the RE program, only 19% of the total households had access to electricity. By 1984 this percentage had increased to around 43% and by 1986 to 86% and by 1990 electrification level was more than 91%. Fig.2 shows the electrification level in Thailand. By the year 2000 percentage of household having access to electricity in rural and urban areas differed by a very small percentage show in Fig. 2.

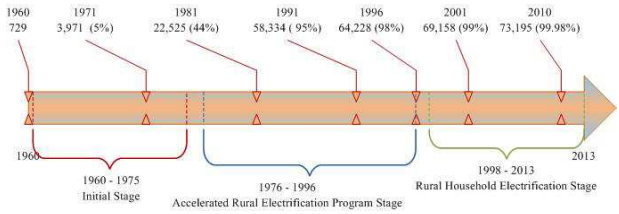

Fig.2. Electrification Level in Thailand

Initial Stage: During 1964-1975, PEA implemented 3 RE Projects by the supply from small diesel power plants to about 10,000 villages and able to achieve 20 % RE. Accelerated Rural Electrification Program Stage: During 1976-1996, the implementation was through a connected to grid system after PEA implemented the accelerated RE Program, the number of Electrification Village increase as follow: 1981: 22,525 Villages (44%), 1986: 41,374 Villages (75%), 1991: 58,334 Villages (95%), 1996: 64,228 Villages (98%).

According to PEA Report in 2012, within 74 provinces under its responsible areas in Thailand, there are a total of 73,363 villages those had access to electricity, which

is equivalent to 99.98% of the total number of villages in country. These covered 99.10% of the total households in the country, which is equal to 16,212,750 households who had access to electricity. However the number of population is growing every year.

2.2 Renewable energy of rural electrification in Thailand

The results study [9] makes a modest attempt, based on extensive literature review, to highlight the rural electrification situation at the regional and country level in South Asia. The significant achievement shows that all the government policy is based on an a priori judgment that renewable energy should be reserved for marginal areas where grid extension is a challenge and so governments are not attempting distributed generation to enhance access utilizing the locally available resources in grid connected areas. Furthermore, based on sustainable development with emphasis on environmental consideration, the feasibility of electrification by using different types of renewable energy such as solar, biomass, hydro, wind and tidal have been studied. Renewable energy is the most promising option for feasible and sustainable decentralized rural electrification generation systems, particularly in rural areas with massive renewable energy resources [6, 10]. Despite reliability of grid connection, results indicate that renewable energy sources are the best choice especially in areas far from grid connections. Challenges between financial institutes and executive agencies result in resource management and technology development in order to overcome existing barriers and issues[11].

Thai government's goal of 25 % renewable energy production by 2021 is an attempt to reduce national dependence on non-domestic energy sources as well as reduction of the environmental burdens associated with domestic energy production[3]. The renewable energy subsidy is very important, Feed in tariffs of USA and Europe are studied to be applies in Thailand[12]. After, NESDP established, PEA's the programme on design, implementation and evaluation for pilot hybrid renewable energy systems for electrification of remote villages. The methodologies used in systems design descriptions and operations of the system was presented in [13]. The technology roadmap of the renewable energy industry was proposed to emphasize the importance[14].In addition, the economic analysis, the capital cost, net present cost, cost of energy and CO_2 emissions were determined for different types of system configuration [15, 16]. Several models of renewable energy resources was proposed by considering daily operation profile[17] and the impact of renewable energy. These models used as a guideline for strategic planning and long-term preparation [18] . The study on the security of primary energy supply for electricity generation in the next 20 years is providing of National Power Development Plan of Thailand (PDP 2010)[19].

2.3 PV Projects in Thailand

The global PV supply chain has rebounded strongly from the overcapacity-induced lows of 2011 to 2013, with robust demand growth from markets such as China, Japan and the U.S. coming into contact with a fitter, leaner supply chain. Tightest PV market supply is expected in 2014 in nearly half a decade, supply constraints and rising input costs are expected to result in meaningful increases in pricing across the PV value chain [20].

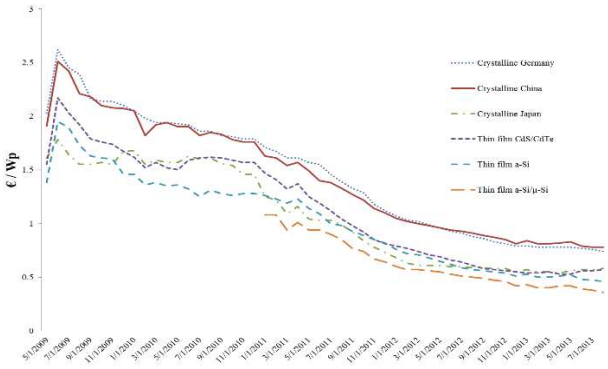

Fig.4 Global PV Pricing Outlook: Q3 2014

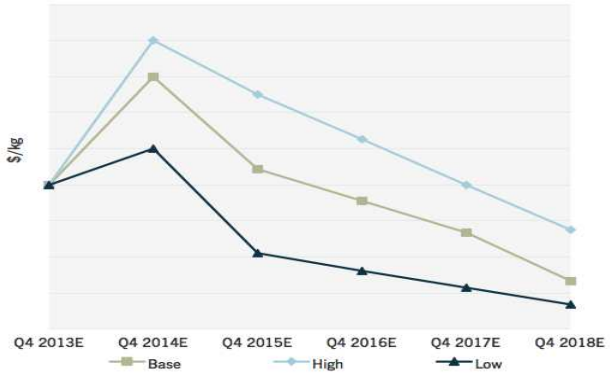

Fig.5 Industry Average Polysilicon Price

The Energy providing that Policy and Planning Office (EPPO) had the survey data, the average prices of solar panels PVX for all the technologies have declined from 1.14 USDW in December 2011 to 0.84 USDW in October 2012 (or 26 percent). While the cost of Solar PV Balance of System (BOS) ago, still does not change those results. Thus the total costs of the project to produce electricity from solar energy reduce from 70.4 million baht per MW. According to the Energy Research Institute proposed the reduction cost of 60 million baht per MW (or about 15 percent). In 2013 the system costs continued to decline by another 7-8 percent, which would make the total cost of system is approximately 55 million baht per MW.

Solar PV technologies serve as a potential supplemental electricity source in Thailand to sell electricity to the grid. Single-crystalline panels have a higher efficiency compared to amorphous silicon and thin-film solar panels, which have a lower cost. The study attempts to reconcile the environmental and economic differences between single-crystalline and thin-film photovoltaic technologies to assist policymakers in the formulation of GHG mitigation strategies [5] . Furthermore, Solar PV systems will be the first priority for renewable energy technology used. Some households many use additional agricultural diesel

for generating electricity in case of energy supply from battery or Solar PV system does not meet energy demand according to the survey results in the rural villages [21].

3 BASIS OF THE ANALYTICAL MODEL

3.1 The Levelized Cost of Energy formula for solar electricity costs

Levelized Cost of Energy (LCOE) are a common metric for comparing power generating technologies. There was criticism particularly towards evaluating variable renewables lie wind and solar PV power based on LCOE because it ignored variability and integration costs [22]. LCOE can be taken of as the price at which energy must be sold to break even over the lifetime of the technology. It yields a net present value in terms of, bath per kilowatt-hour. This is an assessment of the economic lifetime energy cost and lifetime energy production (Eq.1) and it is applicant for any energy technology. In order to compute the financial costs, the equations can be embellished to take into account not only system costs, but also other factors such as financing, insurance, maintenance, and different types of depreciation schedules.

The model calculates the cost of solar electricity during the whole lifetime of the systems, whilst other models estimate that cost annually[23]. The life-cycle technique was applied to estimate the LCOE, the expenses and sales revenues those occur in future time discounted to present time value of money by using discounted cash flow (DCF) techniques, i.e., by calculating the present value of the cash flows by means of a discount rate, r. In this context, the LCOE is determined when the present value of the sum of the discounted revenues is equivalent to the discounted value of the sum of the costs during the economic lifetime of the system, N years, i.e. ,

$$\sum_{n=0}^{N} \frac{Revenues_n}{(1+r)^n} = \sum_{n=0}^{N} \frac{Costs_n}{(1+r)^n} \quad (1)$$

Thus, the Net Present Value (summation of the present values PV of the cash flows), NPV, of the project is zero, i.e.,

$$NPV = \sum_{n=0}^{N} PV = 0 \quad (2)$$

Therefore the LCOE is the averge electricity price needed for Net Present Value (NPV) of zero when performing a discounted cash flow (DCF) analysis, so that an investor would break even and so receive a return proportional to the discount rate of the investment. The sum of the present values of $LCOE_n$ multiplied by the energy generated annually, E_n should be equal to the sum of the present values of the costs of the project, i.e.,

$$\sum_{n=0}^{N} \frac{(LCOE_n)x(E_n)}{(1+r)^n} = \sum_{n=0}^{N} \frac{Costs_n}{(1+r)^n} \quad (3)$$

Assuming a constant annual value for the LCOE, we can write:

$$LCOE = \sum_{n=0}^{N}\left(\frac{Costs_n}{(1+r)^n}\right) / \sum_{n=0}^{N} \frac{E_n}{(1+r)^n} \quad (4)$$

Note that (Eq.4) is an arithmetic result of rearranging (Eq.3) for energy discount. Hence, according to (Eq.4), the LCOE equals to the sum of all the discounted costs incurred during the lifetime of the project divided by the units of discounted energy produced. It should be noted that the summation calculation starts from *n*=0 to include the initial cost of the project at the beginning of the first year, which should not be discounted. Therefore, the initial cost can be included outside the summation and the summation is started from *n*=1 both in the numerator and in the denominator, i.e.,

$$LCOE = \left(Initial\ Costs + \sum_{n=0}^{N}\left(\frac{Annual\ Costs_n}{(1+r)^n}\right)\right) / \sum_{n=0}^{N} \frac{E_n}{(1+r)^n} \quad (5)$$

Finally, the net costs will include cash outflows like the initial investment (via equity or debt financing), interest payments if debt financed, operation and maintenance costs (note: there are no fuel costs for solar PV) and cash inflow such as government incentives as shown in (Eq.6). As such, the net cost term can be modified for financing, taxation and incentives as an extension of the initial definition. If LCOE is used to compare to grid prices, it must include all costs required (including transmission and connection fees if applicable) and must be dynamic with future projects acknowledged in the sensitivity analysis. In this paper, no incentives will be considered [24, 25] .

$$LCOE = \frac{\sum_{n=0}^{N} \frac{IC_n + FOM_n + VOM_n}{(1+r)^n}}{\sum_{n=0}^{N} \frac{E_n}{(1+r)^n}} = \frac{\sum_{n=0}^{N} \frac{IC_n + FOM_n + VOM_n}{(1+r)^n}}{\sum_{n=0}^{N} \frac{S_n(1-d)^n}{(1+r)^n}} \quad (6)$$

where, r = discount rate (%); d = degradation rate (%); n = specified period (year);FOM_n = fixed O&M cost per year (Baht);VOM_n=variable O&M cost per year (Baht);S_n = energy output per year (kWh).

4. SOLUTION METHOD

The energy consumption data of the rural electrification disposition is analyzed by the simulation from the PEA. This paper assigned the average energy unit between 45-112 kwh/month and the PV sizes have 300 w- 750 w of the household. Various prescribed data is the corresponding of the rural electrification in rural area. The sun hour of the PV generation per day is 5 hour/day which is mean value hour in Thailand. There scenarios high, base and low PV investment cost were simulated using global price as parameter as shown in Fig 5. The simulated PV costs show in the Fig.6. The PV costs of which the package price is 100 Baht/Watt are show in Fig. 7 included cost of installation and battery but exclude inverter.

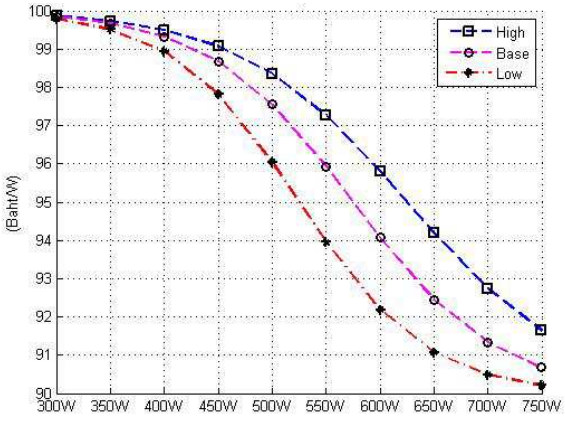

Fig.6 Function Cost PV per watt installed

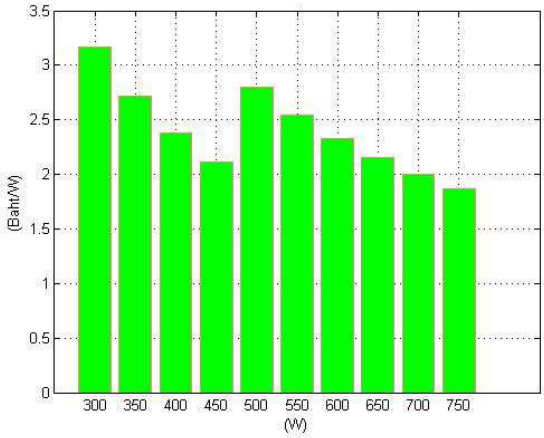

Fig.7 Cost PV inverters per watt installed

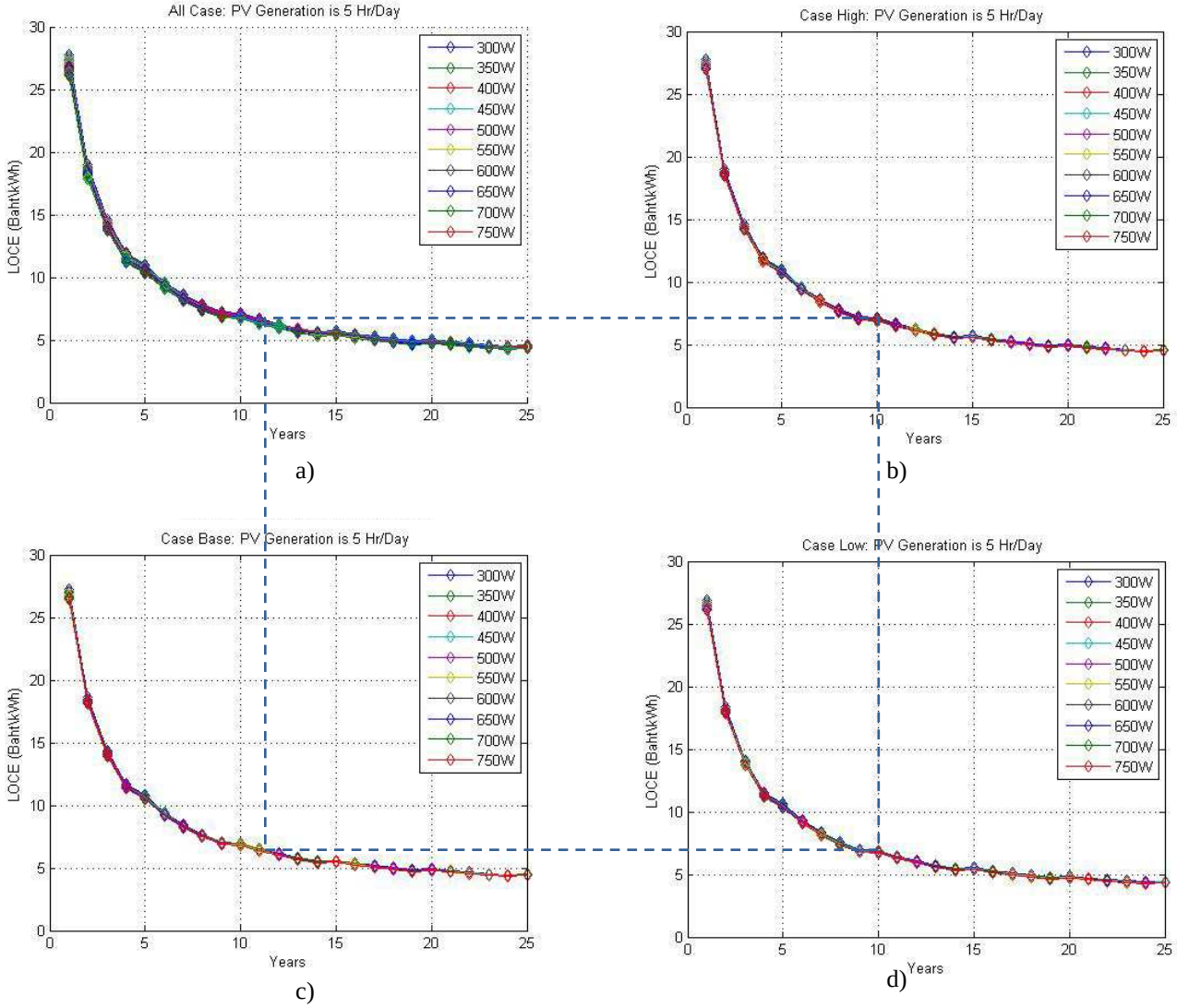

Fig.8 (a) All Case: PV Generation is 5 Hr/Day (b) Case High: PV Generation is 5 Hr/Day(c) Case Base: PV Generation is 5 Hr/Day(d) Case Low: PV Generation is 5 Hr/Day

The parameters simulated for LCOE analysis consisted 1% for the operation and maintenance cost and the inverter and other replacement with expect to the initial cost with the investment carried out every 5 year.

5. RESULTS AND DISCUSSION

The analysis of the PV project (10 years) has the condition that the pv can generate average power of 5 hr/day of year (mean in Thailand). An Analysis of the project is carried out for 10 years, primarily due to

speculation that the project may have problems on other side during this period. The results were shown in Table.2 with the LCOE does not obviously change, but it will result in most of the investments and the life of the project show in the Fig.8.

Table 2. LCOE (5 Hr/Day,Project 10 year)

	High	Base	Low
300W	7.122	6.9964	6.8967
350W	7.074	6.9483	6.8486
400W	7.0379	6.9123	6.8126
450W	7.0099	6.8843	6.7846
500W	6.9875	6.8619	6.7622
550W	6.9692	6.8436	6.7439
600W	6.9539	6.8283	6.7286
650W	6.941	6.8153	6.7156
700W	6.9299	6.8043	6.7046
750W	6.9203	6.7947	6.695

However, the results showed that the factors change LCOE is directly related to the age of the equipment or the life project i.e., the longer life, the lower LCOE value (as shown in Fig.9, Fig.10 and Fig.11, for three scenarios, respectively. While investment equal intervals will be valid for the same but the rates of change of the LCOE not be observed between the life project of 15- 20 years compared 20-25 years, the result that it can be compared to the increase in base tariff of 3.5 Baht / kwh with an annual increase of 3%, with a reduction of the LCOE each year by 0.5%, then we know of suitable for investment

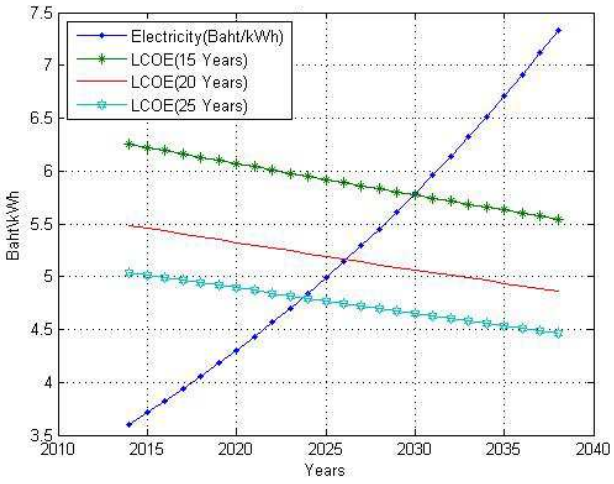

Fig.9. Case High: 500w, 4.6hr/Day.

The analysis to be consistent with the investment currently analyzed to evaluate LCOE in the project 20 years, considering the case different conditions justify the cost of the system has decreased dramatically (Case High), normal price (Case Base) and decreased slowly (Case Low) same as the average cost in the region has decreased by more than 10% of the price in the system. Conclusions are presented in Fig.12, which is divided in two by a conclusion as (a), (c) and (e) shows the results of the LCOE of the PV generation per day, a different part (b), (d) and (f) the effect of the conditions to the investment results of to changes discount rate.

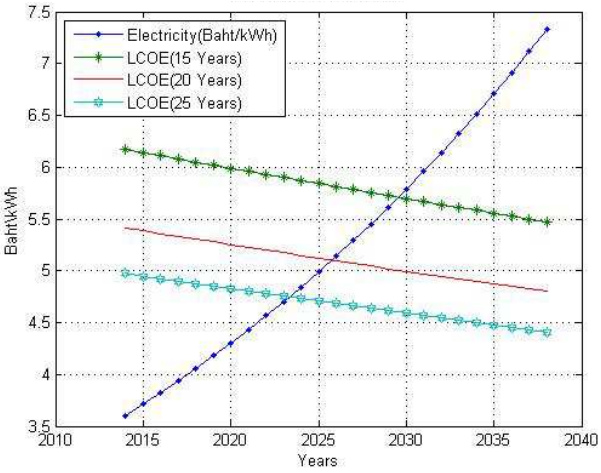

Fig.10 Case Base: 500w,4.6hr/Day.

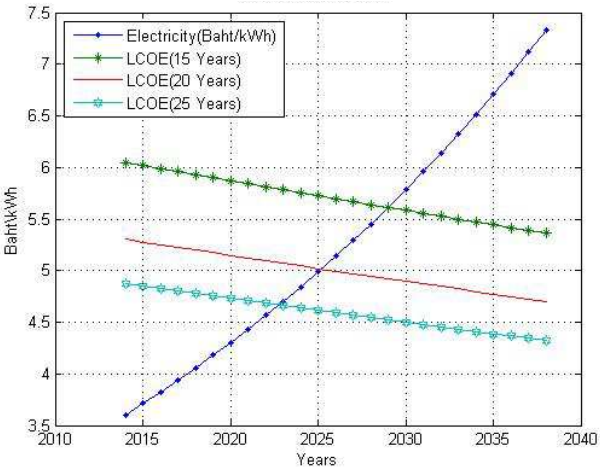

Fig.11 Case Low: 500w,4.6hr/Day

The result of the change in the average hours of electricity per day (considering 3.6 hr / day to 5 hr / day) that the LCOE changes from 5 Baht/kWh to less than 7.5 Baht/kWh and the change of interest rate (the 0.5% to 4%) that the LCOE are the range of 5.7 Baht/kWh to less than 4.6 Baht/kWh overall than in the past, which consider to be the LCOE are much reduced.

The results of the calculations were presented. Under the economic outlook for investment, the authors incorporate the consideration of the current cost of solar cells and the proper average level for rural communities in remote areas. For 25 years investment under the fastest price variation (Case High), the reduction of 10% per annum for PV system investment of 100 Baht/watt and 0.5% increase of base tariff of 3 Baht/kWh could be found. The appropriate year for the investment size of PV household as 500 watt and the PV generate per day is 4.6 hour/day as shown in Fig.10.The appropriate year for investment in the year 2024 that the base tariff and LCOE as 4.84 and 4.80, respectively. It is also noted that for early investment than 2024, it will create over

opposite investment but if the investments was made slowly to the investment opportunities too.

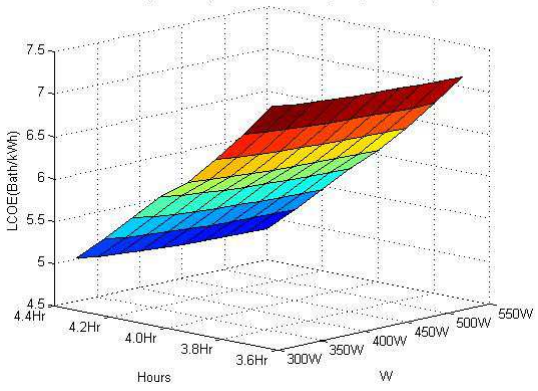

(a)

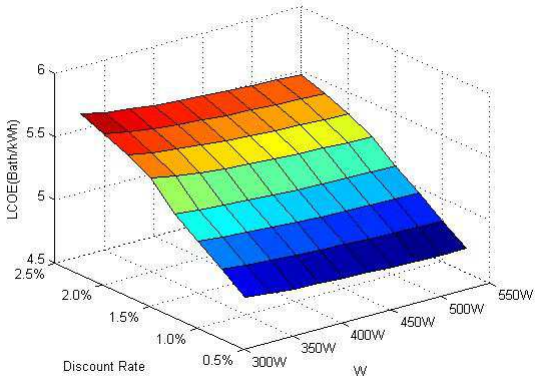

(b)

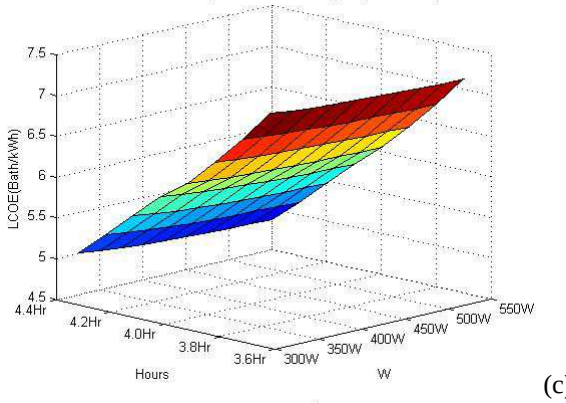

(c)

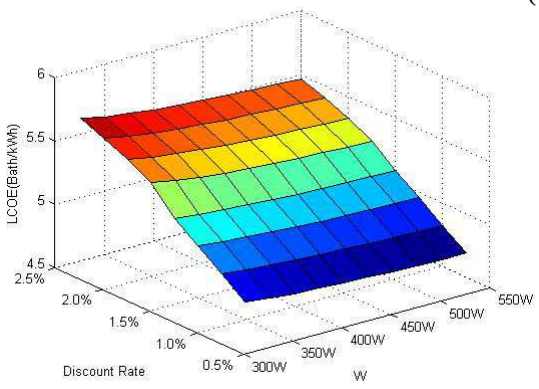

(d)

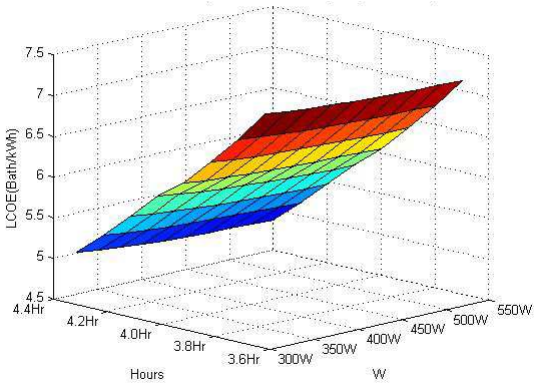

(e)

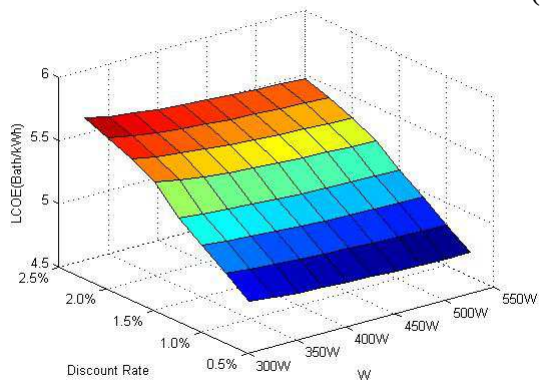

(f)

Fig. 12. (a) Case High: LCOE of PV Generation changes; (b) Case High: LCOE of Discount Rate changes; (c) Case Base: LCOE of PV Generation changes (d) Case Base: LCOE of Discount Rate changes; (e) Case Base: LCOE of PV Generation changes; (f) Case Base: LCOE of Discount Rate changes.

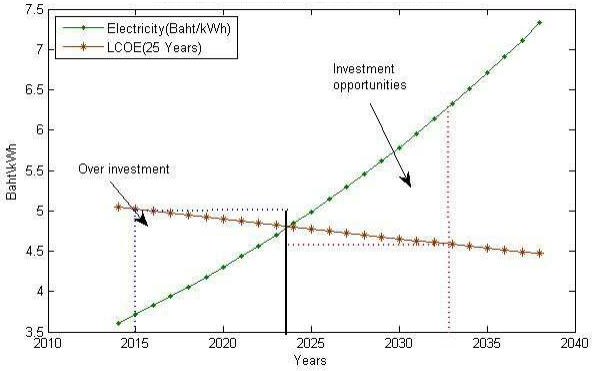

Fig. 13. Case High: LCOE of PV Generation (25 years\500w\4.6Hr).

6. CONCLUSION

In Thailand, the government will make an investment currently invest for RE from PV panels. Both the economy and society needs to be considered. For the economics, dimension real cost of PV systems and if analysis base on reasonable time period there is carried out will not be over-investment and investment opportunities. However, a complete infrastructure in the community to contribute to the economic development in remote communities, causes substantial growth in the overall development of the country and most importantly the conflict in society will be less.

Presently, Thailand has encouraged households with electricity generation from the PV panels as the solar rooftop project, The government will purchase on the feed-in-tariff price and the life have 25 years ,can be connected to the grid system of MEA and PEA. At the same time communities in remote rural areas of the country are not the beneficiaries of the project.

REFERENCES

[1] N. E. A. S. D. Board 2011. The elecventh national economic and social development plan (2012-2016)," Bangkok, Thailand.

[2] Commission E. R. 2012. Power Development Plan 2012-2030 : PDP2010.

[3] Commission, E. R. 2010. Renewable Energy Development Plan: REDP 2008 - 2022.

[4] Commission, E. R. 2010. The Renewable and Alternative Energy Development Plan: AEDP 2012-2021.

[5] Kittner, N., Gheewala, S. H. and Kamens, R. M. 2013, An environmental life cycle comparison of single-crystalline and amorphous-silicon thin-film photovoltaic systems in Thailand. *Energy for Sustainable Development*, vol. 17, pp. 605-614.

[6] Urmee, T., Harries, D. and Schlapfer, A. 2009. Issues related to rural electrification using renewable energy in developing countries of Asia and Pacific. *Renewable Energy*, vol. 34, pp. 354-357.

[7] PEA 1973. National Plan for Thailand Accelerated Rural Electrification.

[8] Chullakesa, C. 1992. Rural Electrification Guidebook for Asia and the pacific. Bangkok, Thailand.

[9] Palit, D. and Chaurey, A. 2011. Off-grid rural electrification experiences from South Asia: Status and best practices. *Energy for Sustainable Development*, vol. 15, pp. 266-276.

[10] Lahimer, A. A., Alghoul, M. A., Yousif, F., Razykov, T. M., Amin, N. and Sopian, K. 2013. Research and development aspects on decentralized electrification options for rural household. *Renewable and Sustainable Energy Reviews*, vol. 24, pp. 314-324.

[11] Javadi, F. S., Rismanchi, B., Sarraf, M., Afshar, O., Saidur, R., Ping, H. W., *et al.* 2013. Global policy of rural electrification. *Renewable and Sustainable Energy Reviews*, vol. 19, pp. 402-416.

[12] Keyuraphan, S., Thanarak, P., Ketjoy, N., and Rakwichian, W. 2012. Subsidy schemes of renewable energy policy for electricity generation in Thailand. *Procedia Engineering*, vol. 32, pp. 440-448.

[13] Kruangpradit, P. and Tayati, W. 1996. Hybrid renewable energy system development in Thailand. *Renewable Energy*, vol. 8, pp. 514-517.

[14] Sarikprueck, P., Korkua, S. K., Wei-Jen, L., and Lumyong, P. 2011. Developing important renewable energies in Thailand. In *Power and Energy Society General Meeting, 2011 IEEE*, pp. 1-8.

[15] Chun-Che, F., Rattanongphisat, W., and Nayar, C. 2001. A simulation study on the economic aspects of hybrid energy systems for remote islands in Thailand. In *TENCON '02. Proceedings and 2002 IEEE Region 10 Conference on Computers, Communications, Control and Power Engineering*, vol.3, p. 1966-1969.

[16] Tanatvanit, S., Limmeechokchai, B., and Chungpaibulpatana, S. 2003. Sustainable energy development strategies: implications of energy demand management and renewable energy in Thailand. *Renewable and Sustainable Energy Reviews*, vol. 7, pp. 367-395.

[17] Chaiamarit, K. and Nuchprayoon, S. 2013. Modeling of renewable energy resources for generation reliability evaluation. *Renewable and Sustainable Energy Reviews*, vol. 26, pp. 34-41.

[18] Nidhiritdhikrai, R., Eua-Arporn, B., and Diewvilai, R. 2012. Impact of renewable energy on Thailand power Development Plan. In *9th International Conference on Electrical Engineering/Electronics, Computer, Telecommunications and Information Technology (ECTI-CON)*, p. 1-4.

[19] Kamsamrong, J. and Sorapipatana, C. 2014. An assessment of energy security in Thailand's power generation. *Sustainable Energy Technologies and Assessments*, vol. 7, pp. 45-54

[20] Mehta, J. J. A. S. (2014). *Global PV Pricing Outlook: Q3 2014*. Available: http://www.greentechmedia.com/research/report/global-pv-pricing-outlook-q3-2014

[21] Yaungket, J. and Tezuka, T. 2013. A Survey of Remote Household Energy Use in Rural Thailand. *Energy Procedia*, vol. 34, pp. 64-72.

[22] Ueckerdt, F., Hirth, L., Luderer, G. and Edenhofer, O. 2013. System LCOE: What are the costs of variable renewables?. *Energy*, vol. 63, pp. 61-75.

[23] Hernández-Moro, J. and Martínez-Duart, J. M. 2013. Analytical model for solar PV and CSP electricity costs: Present LCOE values and their future evolution. *Renewable and Sustainable Energy Reviews*, vol. 20, pp. 119-132.

[24] Branker, K., Pathak, M. J. M. and Pearce, J. M. 2011. A review of solar photovoltaic levelized cost of electricity. *Renewable and Sustainable Energy Reviews*, vol. 15, pp. 4470-4482.

[25] Ranola, J. A. P., Nerves, A. C. and del Mundo, R. D. 2012. An optimal Renewable Portfolio Standard using Genetic Algorithm - Benders' decomposition method in a Least Cost Approach. In *TENCON 2012 - 2012 IEEE Region 10 Conference*, p. 1-6.

Frequency Response for Next Decade Solar Power Development Plan in Thailand Part 1: Frequency Response Model of Thailand Power System

C. Sansilah, P. Bhasaputra and W. Pattaraprakorn

***Abstract*—** *This paper proposes the appropriate frequency response model to analyze the frequency deviation of Thailand power system due to various sizes and location of solar power. Large installed capacity of uncertain solar power will affect power system stability in term of voltage stability and frequency deviation. Existing three types of power plants in Thailand with different automatic frequency control parameters are collected to develop real-time automatic individual power plant parameters tuning (RIPT) frequency response model that can represent frequency response of the whole Thailand power system in dynamic operating conditions. In addition, the RIPT frequency response model is simulated system responses at peaked load operating condition with instantaneous and ramp change in solar power generations. The simulation results show that frequency deviation of each case compare to standard control. Finally, the RIPT frequency response model can be applied to analyze effect of real power and load deviation to power system frequency response for protective planning.*

***Keywords*— Load frequency control, power system of Thailand, renewable power, solar power plant.**

1. INTRODUCTION

Thailand's electricity demand grows about 4.0 percent per year and the estimated demand will become double within the next two decades [1,2] while the main energy source (as shown in Figure 1), natural gas in the gulf of Thailand, is running out of reserves[3]. One dependence source is leading country energy security problem hence use of renewable energy instead of conventional fossil fuel is the most promising solution. However, uncertain energy generation of renewable resource especially solar power significantly affect to power system reliability in term of voltage stability and frequency response. Frequency deviation is unwanted for consumer due that most of AC motors run at speed that are directly related to frequency as well microcontrollers are dependent on frequency for their timely operation. Normally, Thailand's power system frequency is controlled at 50 Hz as the result of controlling all synchronous generators which are performed by the automatic generation control (AGC) system. Nevertheless, instantaneous imbalance of load and generated power during AGC adjustment is to deviate the frequency. According to normal load profile of Thailand, the rapid increasing demand occurs at around 13.00, 15.00 and 20.00 which AGCs response to nominal frequency with a short period of oscillating under frequency not less than 300 MW per 0.1 Hz however at least one time a day the rapid decreasing demand causes the oscillating over frequency. The frequency response of the power system at a specific time of instantaneous changing demand depends on a combination of time constants and AGC's parameters for running individual power plants which are difficultly investigated the actual values and time dependent.

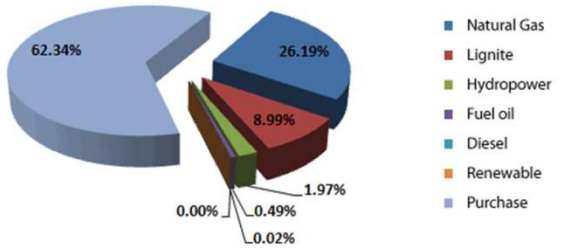

Fig.1. Electrical power generation resources in Thailand (EGAT, 2014)

The generalized load frequency response control (LFC) models are proposed by Kunpur P. [4] and Saadat H. [5] then the modified LFC model for specific power plant types is studied in [6] and renewable energy integration is studied in [6, 7]. Moreover, system inertial frequency response estimations are suggested in [8]. Many recent related researches in frequency respond are proposed and studied through test system [7, 9] or studying influence of solar and wind power integration on frequency dynamic for individual area through various cases with loss of large plant [10]. All of researchers proposed improved LFC model as well as control scheme for system reliability improvement. However, studies of real-world power systems are complicated because the system contains various different types of power plants therefore the appropriate frequency response model is necessary to simulate the effect of unexpected instantaneous deviation of load or

C. Sansilah (corresponding author) is with Department of Electrical Engineering, Faculty of Engineering, Thammasat University, 99 M18 Phaholyothin Road, Khlongluang, Pathumthani, 12120 Thailand. Phone: +66-89-1589-885; E-mail: Chokechais@gmail.com

P. Bhasaputra is with Department of Electrical Engineering, Faculty of Engineering, Thammasat University, 99 M18 Phaholyothin Road, Khlongluang, Pathumthani, 12120, Thailand. E-mail: bporr@engr.tu.ac.th.

W. Pattaraprakorn is with Department of Chemical Engineering, Faculty of Engineering, Thammasat University, 99 M18 Phaholyothin Road, Khlongluang, Pathumthani, 12120, Thailand. E-mail: pworarat@engr.tu.ac.th.

renewable generated power in the system which can support system operator to make prevention plan in order to maintain power system reliability and security.

The main purpose of this study is to investigate impact of large solar power integration on Thailand's power system through considering of frequency response. This paper is a first part to introduce the RIPT frequency response model formulation and another related second part to illustrate simulation result of a PDP 2010 case study. This paper consists of eight sections. Section 1 introduces the research of model LFC. Section 2 is to explain Thailand's power system then basics of power system stability and frequency control are described in section 3 and section 4. Developing frequency response model of Thailand's power system is explained in section 5 then various case studies of load and solar generated power deviation for model examination are described in section 6. Result and discussion of the simulation are presented in section 7. Finally, section 8 is conclusions of this study.

2. THAILAND POWER SYSTEM

Three state enterprise organizations are conducting electrical business in Thailand, the Electricity Generating Authority of Thailand (EGAT) generates and transmits the bulk electricity directly to two distribution authorities, the Metropolitan Electricity Authority (MEA) and the Provincial Electricity Authority (PEA).

Power Generation System

In 2014, EGAT's power plants has a total installed generating capacity of 15,474.13 MW accounting for 44.28 percent of the country's gross energy generation while the purchased power capacity included 13,541.69 MW from domestic independent power producers (IPPs) representing 38.75 percent of the country's total generating capacity 3,524.60 MW or 10.08 percent from small power producers (SPPs) and 2,404.60 MW or 6.88 percent imported from neighboring countries. Proportion of EGAT's power plants classified by types are 10.44 percent of thermal power plant, 23.99 percent of combined cycle power plant, 9.83 percent of hydropower power plant and 0.02 percent of diesel and others power plant as shown in Figure 2.

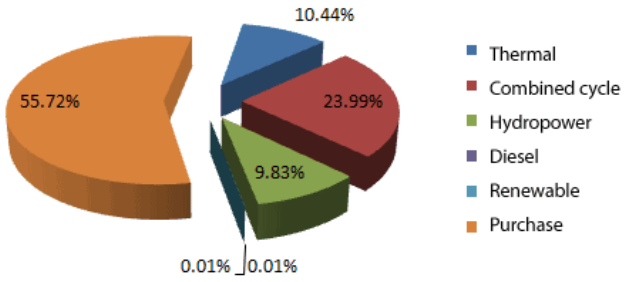

Fig.2. Proportion of EGAT's power plants classify by types (EGAT, 2014)

Transmission Systems

In 2014, Thailand's transmission system consists of 213 substations, 88,036 MVA of transformer capacity and 32,509 circuit-kilometers of transmission line with various voltage levels ranged from 115 kV, 230 kV and 500 kV. The generation and transmission system of Thailand are owned and operated by EGAT via The national control center and five regional control centers. Main power plans and 230/500 kV transmission line of Thailand are showed in Figure 3.

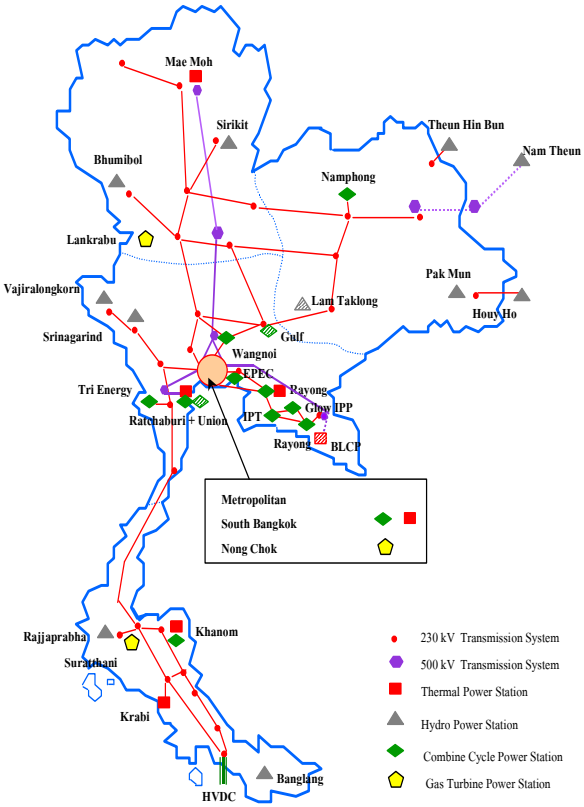

Fig. 3. Main power plans and 230/500 kV transmission line of Thailand.

Electricity Demand of Thailand

In 2014, the peak demand topped 26,942.10 MW on April 23, 2014 at 14.26 marking an increase of 343.96 MW or 1.29 percent from the previous year. In 2013, the net energy totaled 173,535.45 million kWh, 72,113.94 million kWh or 41.56 percent of the country's energy demand was generated by EGAT's power plants, and 101,421.51 million kWh or 58.44 percent were purchased from the private power producers and from neighboring countries.

3. POWER SYSTEM STABILITY

Power system stability is the ability of the power system to maintain the state of operating equilibrium under normal operating conditions and to regain an acceptable state of equilibrium after being subjected to disturbance [3]. The parameters to indicate system stability are system frequency and system voltage. Stability is

generally divided into two major categories, steady state stability and transient state stability. Steady state stability is the ability of power system to regain synchronism after small and slow disturbances. Transient state stability studies deal with effect of large and sudden disturbance such as a fault, sudden outage of a line or sudden application or removal of load [4].This paper focuses on the frequency response of Thailand's power system due to large disturbance of solar power generation.

4. POWER SYSTEM FREQUENCY CONTROL

A power grid requires generation and load closely balance moment by moment therefore, frequent adjustments to the output of generators are necessary. The balance can be judged by measuring the system frequency; increasing of frequency, more power is being generated than used, and all the machines in the system are accelerating. Decreasing of frequency, more load is on the system than the instantaneous generation can provide, and all generators are slowing down. The operating principle of controlling system frequency is controls mechanical energy that applied to turbine of the generator which system frequency is directly related with revolution speed of the rotor. Thus, controlling frequency is controlling the revolution speed of the generator's rotor. Figure 4 insulates a block diagram of load frequency control system (LFC). Generally, large interconnected power system frequency is controlled by the Model energy control centers (MEC).

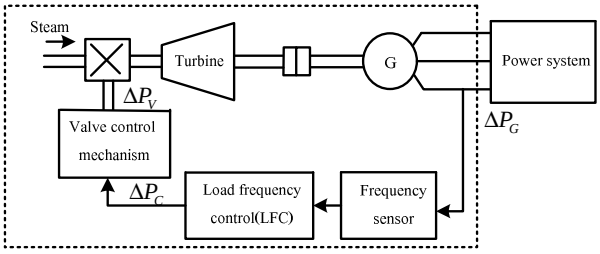

Fig. 4. Block diagram of load frequency control system for *N* generator in power system.

5. FREQUENCY RESPONSE MODEL OF THAILAND POWER SYSTEM

Mathematical modeling of frequency control system in this study is conducted by the transfer function method which is obtained for the following components.

Genorator and Load Model

The frequency deviation ($\Delta\Omega$) under influence of inertia of turbine and generator (inertia constant, H) caused by unbalance of electrical power (P_e) and the mechanical power (P_m) during a small disturbance is define as equation 1.

$$\Delta\Omega(s) = \frac{1}{2Hs}\left[\Delta P_m(s) - \Delta P_e(s)\right] \tag{1}$$

The overall frequency-dependent characteristic of composite load in the system may be expressed as;

$$\Delta P_e = \Delta P_L - D\Delta\omega \tag{2}$$

where ΔP_L is resistive load change, $D\Delta\omega$ is reactive load change and D is load-damping constant which is expressed as a percent change in load for one percent change in frequency.

Turbine Model

The model for nonreheat steam turbine relates change in mechanical power output (ΔP_m) to change in steam valve position (ΔP_V) can be approximated with a single time constant τ_T as;

$$\Delta P_m(s) = \frac{1}{1+\tau_T s}\Delta P_V(s) \tag{3}$$

Governor Model

In order to stable load division between two or more generators operating in parallel, the governors are provided with a characteristic so that speed drops as the load increase. The governor model can be defined as equation 4.

$$\Delta P_V(s) = \frac{1}{1+\tau_g}[\Delta P_{ref}(s) - \frac{1}{R}\Delta\Omega(s)] \tag{4}$$

where τ_g is time constant for the governor, ΔP_{ref} is the reference power change and *R* is speed regulation of the governor which is the ratio of frequency deviation to change in power output in percentage.

The Isolated Power System

Combining mathematic models from equation 1-4 results in the block diagram of frequency control model for isolated power system, as shows in Figure 5 and the close-loop transfer function relating the load change (ΔP_L) to the frequency deviation ($\Delta\Omega$) is shows in equation 5

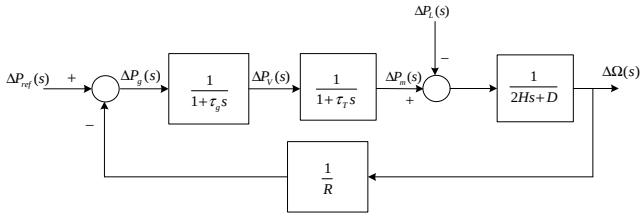

Fig. 5. Block diagram of frequency control model for isolated power system.

$$\frac{\Delta\Omega(s)}{-\Delta P_L(s)} = \frac{(1+\tau_g s)(1+\tau_T s)}{(2Hs+D)(1+\tau_g s)(1+\tau_T s)+\frac{1}{R}} \tag{5}$$

The Isolated Power System with AGC

In order to reduce frequency deviation to zero, the integral controller is added to the model as show in Figure 6 and the close-loop transfer function equation 6

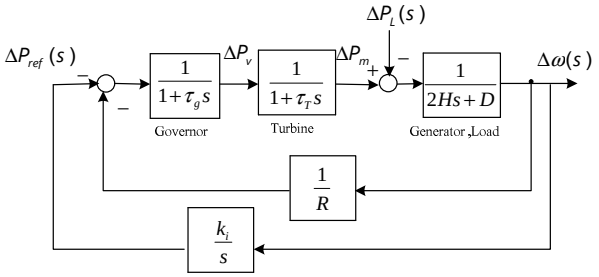

Fig. 6. Block diagram of frequency control model for isolated power system with integral controller.

$$\frac{\Delta\Omega(s)}{-\Delta P_L(s)} = \frac{s(1+\tau_g s)(1+\tau_T s)}{s(2Hs+D)(1+\tau_g s)(1+\tau_T s)+k_i+\frac{s}{R}} \quad (6)$$

The equivalent Isolated Power System for multi-generaters

The equivalent isolated power system for multi-generators model assumes that the coherent response of all generators to change in system load and represent them by an equivalent generator which an inertia constant (H_{sys}) equals to the sum of the inertia constants of all generators. Similarly, a single damping constant (D_{sys}) is represented the effect of system loads. The block diagram of the model shows in Figure 7 which parameters are defined as, $\tau_{g1}...\tau_{gN}$ are time constant of governors 1 to N, $\tau_{t1}...\tau_{tN}$ are time constant of turbines 1 to N, $k_{g1}...k_{gN}$ are gain constant of governors 1 to N, $k_{t1}...k_{tN}$ are gain constant of turbine 1 to N, $R_1...R_N$ are speed regulating of governors 1 to N and k_i is grain constant of integral control unit.

RIPT Frequency Response Model

The real-time automatic individual power plant parameters tuning (RIPT) frequency response model is the time-dependent model based on amounts, types and capacities of online-generators at a considered time. According to numerous unknown parameters in the system, all possible typical ranges of individual power plant parameters are used for running in model to find out reasonable model that can represent frequency response characteristic of the system.

RIPT model simulates the isolated power system which is parallel connection of 105 power generators with 4 groups of power plant types, 47 generators of hydro power plants, 17 generators of thermal power plants, 14 generators of combined cycle power plant and 27 generators of IPP's combined cycle power plant.

6. SIMULATION CASE STUDIES

Operating Condition

Frequency response of power system at a specific time depends on various combination types of power plants which are operating at that time. The system operators have to optimize operating cost with acceptable reliability. Thus, the most economical thermal power plants are base load power plants while combined cycle and IPPs power plant are supported for intermediate load level and Hydro power plants are reserving for peaked load etc.

In this study, RIPT frequency respond model of Thailand's power system is examined by peaked load operating condition which all generators are running as shows in Table 1.

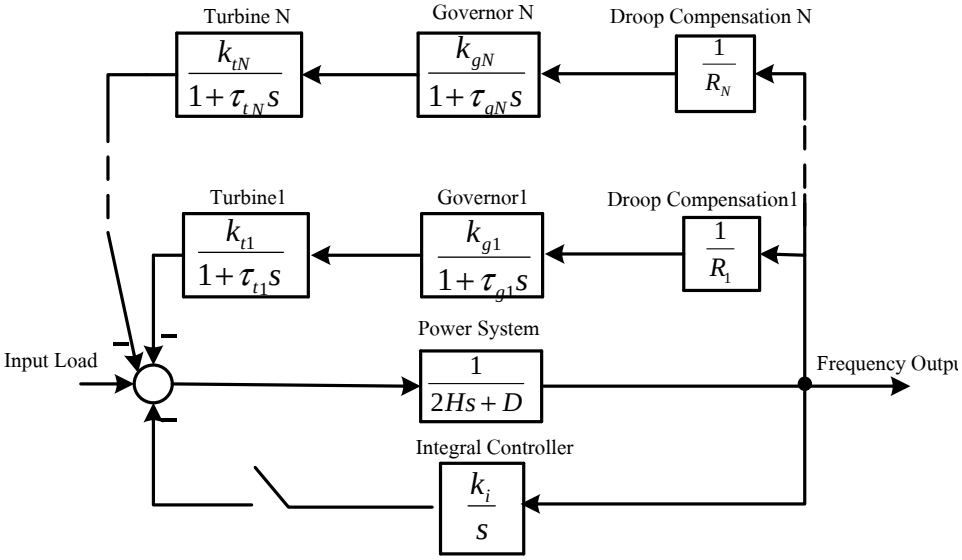

Fig.7. Block diagram of the isolated power system equivalent for multi-generator

Table 1. Number of online-generator of peaked load condition

Group of generator	Number of generators	Installed capacity (MW)	Percentage
Hydro	47	3,391	10.7
Thermal	17	5,615	17.7
Combined cycle	14	7,926	25.0
IPPs	27	14,760	46.6
Total	105	31,692	100.0

Model Parameter Tuning

According to discover an appropriate frequency response model, all possible values of unknown parameter sets such as the inertia constant (H_{sys}), damping constant (D_{sys}) and gain constants of turbine and governor etc., are used to run in the RIPT frequency response model. Over 43,923 cases of results are screened and classified into 3 models, the strong system model, the near actual system model and the weak system model.

Variation of Solar Power

Depending on the aggregation level and geographic diversity, solar plants output can decrease/increase within a range of 20%-80% of capacity at 1 min interval [11]. Therefore, the examination assumes that the solar power deviation at average rate, 40 % (300 MW) of the existing 780 MW capacity. The examination cases are divided into 3 cases;

1) Step decrease/increase of solar power by 300 MW
2) Ramp decrease/increase of solar power by 300 MW in 30 seconds
3) Step decrease of solar power by 300 MW with outage of the 700 MW of conventional power plant

7. SIMULATION RESULTS

The developed RIPT frequency response models consist of 3 different tuned parameter sets under assumption of the strong system model, the near actual system model and the weak system model. The results of simulation performed though multi-scenarios of solar power change are present as below.

Case1: Step decrease/increase of solar power by 300 MW

The effective step decrease of solar power by 300 MW shows in Figure 8. According to the graph, the upper line, the middle line and the lower line represent frequency response of the strong system model, the near actual system model and the weak system model, respectively. Considering on the strong system model, without AGC, the steady state system frequency is dropped from 50 Hz to 49.96 Hz at the different -0.04 Hz which in normal frequency control range (±0.1 Hz). Similarly, the steady state frequency of the near actual system model is dropped from 50 Hz to 49.90 which is on the normal control limit. However, the steady state frequency of the weak system model is dropped 0.21 Hz which is out of range for emergency control.

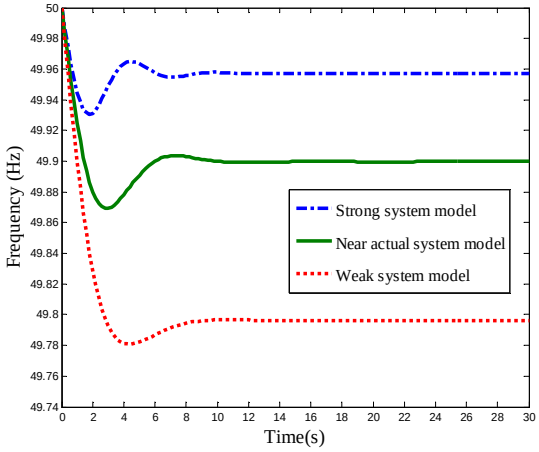

Fig. 8. Frequency response due to step decrease of solar power by 300 MW.

The effective step increase of solar power by 300 MW is shown in Figure 9. In contrast of frequency response of previous case, without AGC, the steady state system frequency of strong, near actual and weak system model are increased from 50 Hz to 50.04 Hz, 50.10 Hz and 50.21 Hz, respectively. A case of weak system model is out of range for normal control.

Case 2: Ramp decrease/increase of solar power by 300 MW in 30 seconds

The effective ramping decrease of solar power by 300 MW in 30 seconds shows in Figure 10. According to the graph, the lower line, the middle line and the upper line represent to the system frequency without AGC of strong, near actual and weak system model, respectively. The result shows that system frequency is slowly decreased from 50 Hz to steady state at 49.96 Hz, 49.90 Hz and 49.79 within about 35 seconds for strong, near actual and weak system model, respectively. A case of weak system model is out of range for normal control.

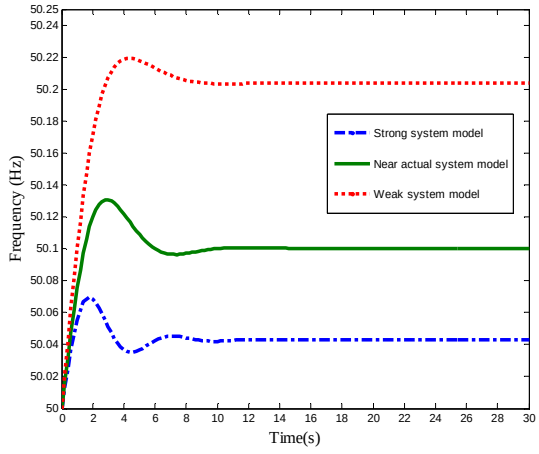

Fig. 9. Frequency response due to step increase of solar power by 300 MW.

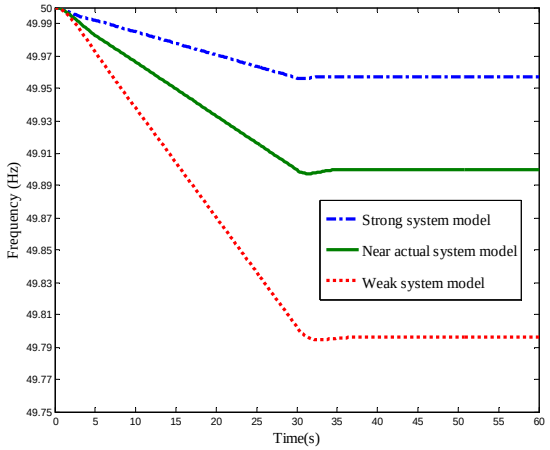

Fig. 10. Frequency response due to ramping down of solar power by 300 MW in 30 seconds.

The Figure 11 shows frequency responses due to step increase of solar power by 300MW in 30 seconds. The system frequency without AGC of the weak system model is out of range for normal control.

Case 3: Step decrease of solar power by 300 MW with outage of the 700 MW of conventional power plant

The results of frequency responses due to the worst case scenario, the step decrease of 300 MW solar power with outage of the largest online-generator (700 MW) are presented in Figure 12, without the AGC, the steady state frequency are dropped from 50 Hz to 49.85 Hz with 0.15 Hz of difference, 49.65 Hz with 0.35 Hz of difference, and 49.30 Hz with 0.70 Hz of difference for strong, near actual and weak system model, respectively. All of 3 models are out of range for normal control.

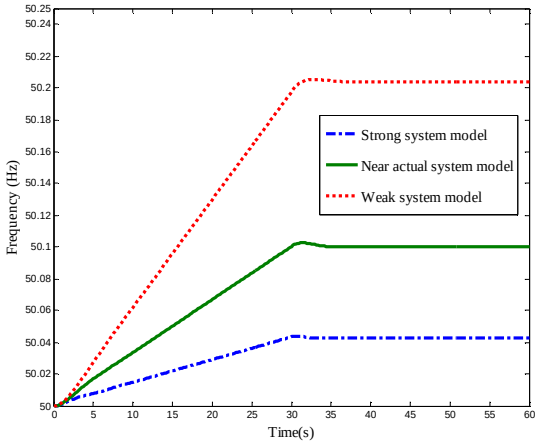

Fig. 11. Frequency response due to step increase of solar power by 300MW in 30 seconds.

From the simulation results, solar development plan in Thailand needs the dynamic model to evaluate frequency response; however the accurate real-time model is very complicated to develop under the actual conditions. In addition, most of frequency response researchers are not interested in the effect of solar power plant in long term planning.

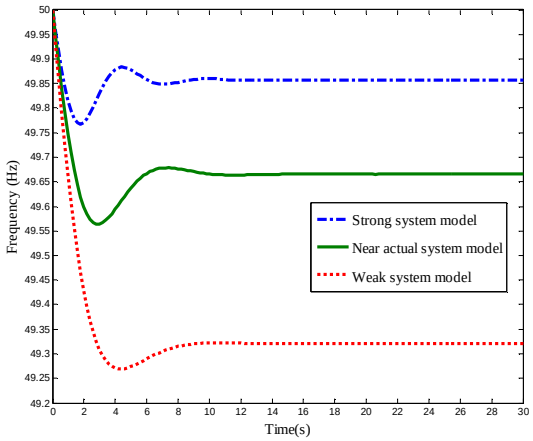

Fig. 12. Frequency responses due to step charge of solar power by 300 MW with outage of the largest generator 700 MW.

8. CONCLUSIONS

The enhancing sustainable energy development introduces large solar power plants to Thailand's power system therefore studying their impacts on system stability are important for regulator and system operator to make the regulation and prevention plan. This paper proposes the RIPT frequency response model to analyze the frequency deviation due to uncertain solar power. The model is simulated the load frequency control system for 105 generators divided into 4 groups which consist of 47 hydro power generators, 17 thermal generators, 14 EGAT's combined cycle generators and 27 IPP's combined cycle generators. The time dependent RIPT frequency response model is examined by a peaked load operating condition which is operated all of generators in the systems under multi-scenario of solar power changes with outage of a 700 MW of conventional generator.

The results show that in case of solar power change at 300 MW instantaneously, and slowly change at 300 MW in 30 seconds, the frequency deviation of the strong system model and the near actual model stay in normal frequency control. However, in case of the weak system model, frequency deviation is 0.2 Hz and out of range for the normal control. The near actual model can be handled the 300 MW of solar power step change however when the 700 MW biggest unit outages, normal frequency control is out of range. In the next part of the paper will present the frequency response for next decade solar power development plan in Thailand by using the proposed real-time automatic individual power plant parameters tuning frequency response model.

ACKNOWLEDGEMENT

This research was supported by Faculty of Engineering, Thammasat University.

REFERENCES

[1] Energy Policy and Planning Office, Ministry of Energy, Thailand (2014). Power Development Plan 2010 Revision 3.

[2] Department of Alternative Energy Development and Efficiency 2012. The Renewable and Alternative Energy Development Plan for 25 Percent in 10 Years (AEDP 2012-2021).

[3] BP Statistical Review of World Energy 2014. [On-line] Avalible on: http://www.bp.com/content/dam /bp/pdf/ Energy- economics/statistical-review-2014 [Oct 10, 2014].

[4] Kunpur P. 1991. Power system stability and control, McGraw-Hill, Englewood Cliffs, NJ.

[5] Saadat, H. 1999. Power System Analysis. McGraw-Hill.

[6] Gillian L., Julia R., Damian F. and Mark J. O'Malley 2005. Power Systems: The Impact of Combined-Cycle Gas Turbine Short-Term Dynamics on Frequency Control, vol. 20, No. 3, pp. 1456-1464.

[7] Bevrani H. 2009. Robust power system frequency control. Springer, New York.

[8] Lisa R., Nicholas W. Jonathan O and Damian F. 2012. Sustainable Energy. Frequency Response of Power Systems with Variable Speed Wind Turbines, vol. 3, no. 4, pp. 683-691.

[9] Bevrani H., Ghosh A. and Ledwich G. 2010. Renewable energy sources and frequency regulation: survey and new perspectives. *IET Renewable Power Generation*.

[10] Sandip S, Shun H. H. and NDR Sarma. System Inertial Frequency Response Estimation and Impact of Renewable Resources in ERCOT Interconnection, Electric Reliability Council of Texas (ERCOT, Inc), USA.

Frequency Response for Next Decade Solar Power Development Plan in Thailand Part 2: A Case Study of PDP 2010 Version 3

C. Sansilah, P. Bhasaputra and W. Pattaraprakorn

Abstract*— *This paper studies the impacts of large solar power installations on frequency responses of Thailand's power system according to the power development plan (PDP 2010 version 3) by considering three levels of electrical demand; light load, partial peaked load and peaked load; during available solar power generation. In addition, the selected actual solar power generation patterns from large solar power plant are collected to analyze the average solar power output and maximum deviation. The frequency responses are simulated by using the proposed real-time automatic individual power plant parameters tuning (RIPT) frequency response model to indicate the effect of installed solar power plants from PDP with various cases in term of the maximum frequency deviations for the next fifteen years. Furthermore the system frequency deviations of each cases are the results of combination of different power plant types and parameter settings, which are compared to each other and the frequency standard control. Finally, the outcomes can be utilized to make prevention plans in order to maintain power system reliability and security for sustainable power development plan with solar power plants.

***Keywords*— Load frequency control, power system of Thailand, renewable power, solar power plant.**

1. INTRODUCTION

Thailand Power Development Plan 2010 - 2030 (PDP 2010 version 3) is targeted on increasing share of solar power by 3,940 MW at the end of 2030, in order to successfully develop sustainable energy production [1-2]. However, the new challenges for power system operators are to control and manage system reliability for both short-term and long-term, the system operators have to consider the influence of uncertain solar power generation which may significantly affect to power system reliability especially in term of frequency deviation. Generally, decreasing solar power generations due to weather conditions, will drop the system frequency because of the imbalance between generation and load. Normally, Thailand's power system is controlled frequency at 50 Hz by the automatic generation control (AGC). The ability to maintain frequency of the system depends on characteristics of the power system at considering time which concerned the combination of online-generator types and its parameter settings. Therefore, the frequency response simulation is necessary to investigate effective solar power deviation that the results can support system operator to make prevention plan in order to maintain power system reliability.

C. Sansilah (corresponding author) is with Department of Electrical Engineering, Faculty of Engineering, Thammasat University, 99 M18 Phaholyothin Road, Khlongluang, Pathumthani, 12120 Thailand. Phone: +66-89-1589-885; E-mail: Chokechais@gmail.com

P. Bhasaputra is with Department of Electrical Engineering, Faculty of Engineering, Thammasat University, 99 M18 Phaholyothin Road, Khlongluang, Pathumthani, 12120, Thailand. E-mail: bporr@engr.tu.ac.th.

W. Pattaraprakorn is with Department of Chemical Engineering, Faculty of Engineering, Thammasat University, 99 M18 Phaholyothin Road, Khlongluang, Pathumthani, 12120, Thailand. E-mail: pworarat@engr.tu.ac.th.

The generalized load frequency response control (LFC) models are proposed by Kunpur P. [4] and Saadat H. [5] then the modified LFC model for specific power plant types is studied in [6] and renewable energy integration are studied in [6, 7]. Moreover, system inertial frequency response estimations are suggested in [8]. Many recent related researches in frequency respond are proposed and studied through test system [7, 9] or studying influence of solar and wind power integration on frequency dynamic for individual area through various cases with loss of large plant [10]. All of researchers proposed improved LFC model as well as control scheme for system reliability improvement. However, studies of real-world power systems are complicated because the system contains various different types of power plants.

The main purpose of this study is to investigate impact of large solar power integration on Thailand's power system through considering frequency deviation. This paper is a second part to illustrate simulation result of a PDP 2010 case study and another related part to introduce the RIPT frequency response model formulation. In this study, various cases of integrations of conventional power plants and solar power plants from the PDP 2010 version 3 will be simulated through the RIPT frequency response model.

This paper consists of six sections. Section 1 introduces the research of frequency control. Section 2 shows the collected data of the selected actual solar power generation patterns from large solar power plant and the analyzed data for frequency response simulation. Then PDP 2010 version 3 is described in section 3 and section 4 explains more details about three levels of electrical demand during available solar power generation and annual solar power deviation of PDP then the simulation results of the frequency response in term of the maximum frequency deviations for the next fifteen years are discussed in section 5. Finally, the conclusion

of this study and recommend on power system reliability and security for sustainable power development plan with solar power plants will be presented in section 6.

2. IMPACTS OF SOLAR POWER PLANTS

Solar power plants convert the solar irradiance of the sun into electric power. Thus, any variations in the solar irradiance lead to fluctuations in the generated output power. The time period of fluctuations can range from few seconds to few hours depending on the wind speed, the type and size of passing clouds, and the area of the solar power plant. Therefore, the time period for collecting the solar power output should be accurate for frequency response simulation. Figure 1 shows the fluctuation of solar power output every minute during daytimes. The different lines represent solar irradiance for different weather and the sky conditions such as sunny, partly sun and cloud and fully cloud. Depending on the aggregation level and geographic diversity, solar plants output can decrease/increase within a range of 20%-80% of its capacity at 1 min interval [3].

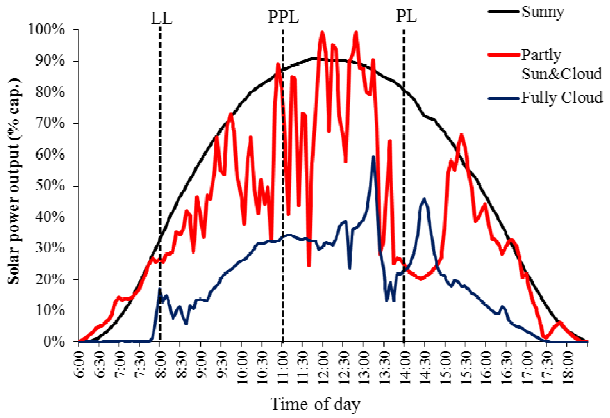

Fig.1. Variation of solar power output

Table 1. The average solar power output and the maximum deviation

Solar power output	LL (8:00) (% cap.)	PPL (11:00) (% cap.)	PL (12:00) (% cap.)
Average	22.92	62.09	48.15
Maximum deviation	16.71	45.28	35.12

There are several factors that dominate the severity of solar power impacts on the power system, some of these factors are type of clouds, location of the solar power plant, installed capacity of the solar power plant, characteristic of the solar power plant and characteristic of the power system. The purpose of this study is to investigate solar power impacts for the preventive planning and the worst case assumption of solar power generations. The maximum deviations of solar output at each considering time, light load at 8.00 (LL), partial peaked load at 11.00 (PPL) and peaked load at 14.00 (PL) as shown in Table 1, are used to calculate the step changes of solar powers, based on installed capacity of solar power from the PDP 2010 version 3.

3. POWER DEVELOPMENT PLAN OF THAILAND

Thailand's Power Development Plan (PDP), is the master investment plan for power system development. The themes of PDP 2010 substantially focused on security and adequacy of power system, environment concern, energy efficiency and renewable energy promotion. The PDP targeting on increasing share of renewable energy and alternative energy uses by 25 percent instead of fossil fuels within the next 10 years, new projects of renewable energy development are initiated into PDP2010 version 3. Hence, at the end of 2030, total capacity of solar power will be up to 3,940 MW or 5.6 percent of total generating capacity in the power system comprising total existing capacity amounting 138 MW, total added capacity of renewable energy of 3,802 MW [1] that is equal to 2,755 percent increasing as shown in Table 2 and Figure 2. According the PDP 2010 version 3, this study will investigate the impacts of increasing uncertain solar power.

Table 2. Capacity of renewable energy as PDP 2010

Type	As of 2011	Additional (2012-2030)	Grand Total
Solar	138	3,802	3,940
Wind	3	1,974	1,977
Hydro	5,323	5,804	11,127
Biomass	747	2,602	3,350
Biogas	106	46	152
MSW	21	352	374
Tides &Waves	2	-	2
Total	6,340	14,580	20,920

Fig.2. Capacity of solar power from PDP 2010 version 3

4. PDP 2012 CASE STUDY

RIPT Frequency Response Model

The real-time automatic individual power plant parameters tuning (RIPT) frequency response model is the time-dependent model based on amounts, types and capacities of online-generators at a considered time. According to numerous unknown parameters in the system, all possible typical ranges of individual power plant parameters are used for running in model to find out reasonable model that can represent frequency response characteristic of the system. RIPT model simulates the isolated power system which is parallel connection of 105 power generators with 4 groups of power plant types, 47 generators of hydro power plants, 17 generators of thermal power plants, 14 generators of combined cycle power plant and 27 generators of IPP's combined cycle power plant.

Generators Operating Condition

Frequency response of power system at a specific time depends on various combination types of power plants which are operating at that time. The system operators have to optimize operating cost with acceptable reliability. Thus, the most economical thermal power plants are base load power plants while combined cycle and IPPs power plant are supported for intermediate load level and Hydro power plants are reserving for peaked load etc. In this study, RIPT frequency response model of Thailand's power system is used to simulate the frequency of 3 operating conditions as following.

1) Light load operating condition (LL)
2) Partial peaked load operating condition (PPL).
3) Peaked load operating condition(PL)

The summary number of operating generators of each case shows in Table 4.

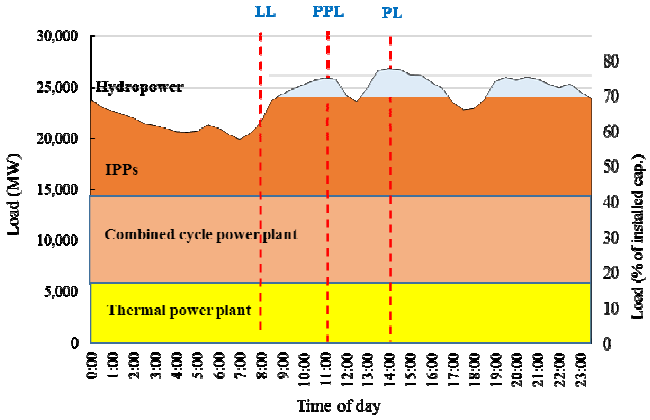

Fig. 3. Power plant operation base on electricity demand.

Table 3. Solar power deviation of each case study

Year	Total cap. (MW)	Solar cap. (MW)	Maximum step change of solar and load combination (MW)					
			LL		PPL		PL	
			Decrease	Increase	Decrease	Increase	Decrease	Increase
2014	39,542	860	179	113	347	427	292	310
2015	43,157	1,051	215	143	429	517	358	378
2016	45,530	1,181	239	163	485	578	403	424
2017	47,240	1,311	262	183	542	638	448	470
2018	48,329	1,441	285	205	600	697	493	515
2019	51,386	1,592	314	228	664	768	546	569
2020	50,389	1,743	338	254	733	835	599	622
2021	52,912	1,944	375	286	821	928	668	692
2022	56,135	2,164	415	321	917	1,031	745	770
2023	56,732	2,384	453	358	1,016	1,130	822	847
2024	59,509	2,604	492	393	1,112	1,232	898	925
2025	60,477	2,824	531	430	1,210	1,332	975	1,002
2026	64,007	3,045	571	464	1,306	1,435	1,051	1,080
2027	64,979	3,266	609	501	1,404	1,535	1,128	1,158
2028	67,012	3,487	649	537	1,501	1,637	1,205	1,236
2029	69,358	3,710	688	573	1,599	1,739	1,283	1,314
2030	70,686	3,940	729	611	1,701	1,844	1,363	1,395

Table 4. Number of on-line generators of each scenario

Group of generators	Number of on-line generators		
	LL (8:00)	PPL (11:00)	PL (14:00)
Hydropower	-	20	47
Thermal	17	17	17
Combined cycle	14	14	14
IPPs	15	27	27
Total	**46**	**78**	**105**

Solar Power Variation Based on PDP 2010

The assumption of solar power change for the simulation based on installed capacity of solar power plants according to the PDP 2010 version 3 is presented in Table 3. In case of LL, the average solar power output is 22.9 percent of installed capacity and the maximum deviation is 16.71 percent of install capacity. Similarly, in case of PPL and PL, average solar power outputs and maximum deviations are presented in Table.1

5. SIMULATION RESULTS

In normal conditions, the system frequency is controlled within ±0.1 Hz either side of 50 Hz then out of this range are emergency control range. This section presents the maximum frequency deviations of the LL, PPL and PL operating conditions due to combination of solar power and load changes based on the solar power installed capacity of each year and the maximum solar power deviations as shown in Table 3.

Frequency Response of Light Load (LL)

The LL conditions occur at 8.00 o'clock that the solar power plants can produce the average power outputs 22.92 percent of their installed capacities then the power changes are less than in case of PPL and PL. Considering Figure 4, in case of solar power decrease, the steady state frequency of year 2020 and 2030 are out of normal control range. On the other hand, in case of solar power increase, only the frequency of year 2030 is out of normal control range while the frequency of year 2020 is stayed in normal control range because of load increase at this moment. Note that the AGC is needed in case of the frequency out of normal control range.

Frequency Response of Partial Peaked Load (PPL)

In PPL, steady state frequencies of all years are out of normal control range (as see in Figure 5) because there are large changes of solar power and load in this moment. In this study, the worst case of solar power fluctuation, 73 percent of its capacity is assumed although in real situation, the occurrence probability are less than 0.1 percent. However, the frequency of year 2014 will be in normal control range in case of the maximum fluctuation of solar power less than 30 percent of its install capacity.

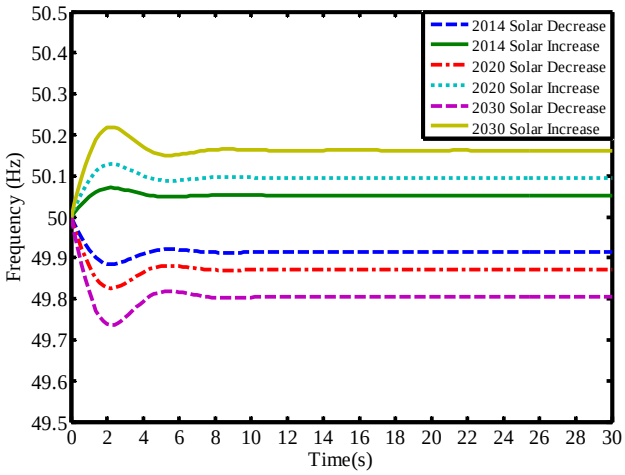

Fig. 4. Frequency response of LL for the years 2014, 2020 and 2030.

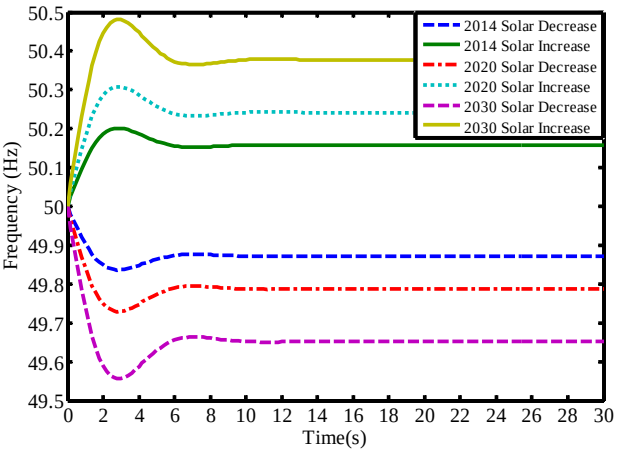

Fig. 5. Frequency response of PPL for the years 2014, 2020 and 2030.

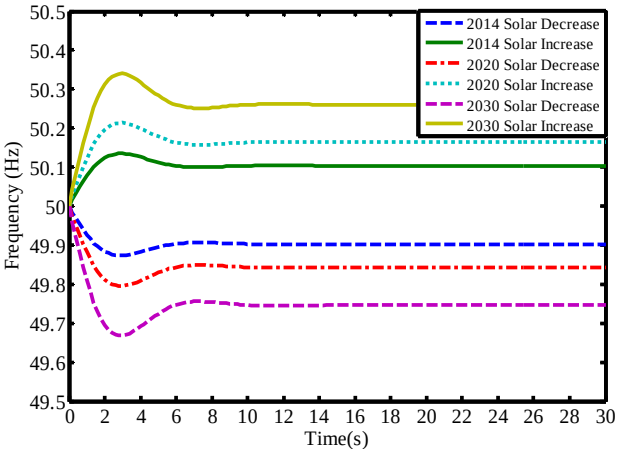

Fig. 6. Frequency response of PL for the years 2014, 2020 and 2030.

Frequency Response of Peaked Load (PL)

The PL operating condition represents for stronger power system because there are more numbers of online-generators can be handle power changes. In year 2004,

the frequency deviations due to change of solar power and load are less than normal control allowance while the frequencies for year 2020 and 2030 are out of normal control as seen in Figure 6.

Frequency Response of the Worst Case in Year 2030

The frequency responses of worst cases the in year 2030 which is the highest installed capacity of solar, for LL, PPL and PL operating condition are represented in Figure 7, 8 and 9, respectively. In case of on AGC, the steady state frequencies of all condition are out of normal control range. With AGC control the frequencies are regaining to nominal frequency (50 Hz) with in 15, 13 and 18 seconds for LL, PPL and PL, respectively.

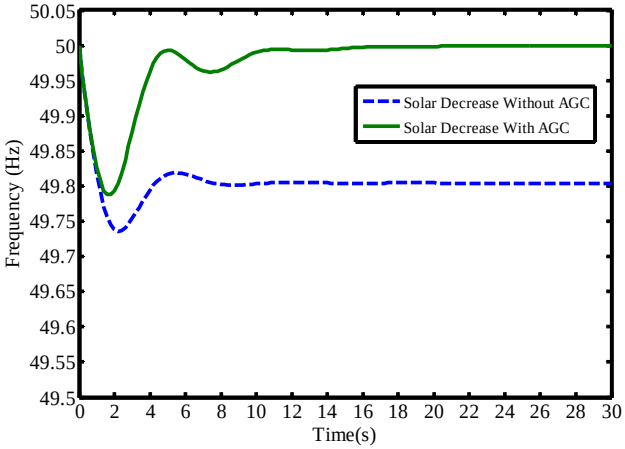

Fig. 7. Frequency response of LL with and without AGC.

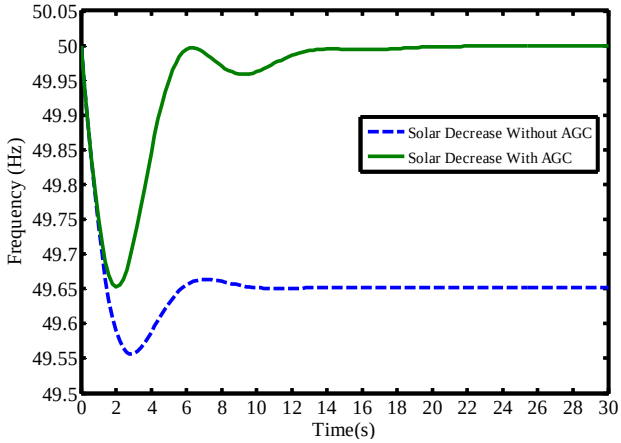

Fig. 8. Frequency response of PPL with and without AGC.

Considering on Figure 8 which represents for frequency response of PPL due to step decrease by 1,701 MW of solar power in the year 2030, the total 3940 MW of solar power plans are installed. The steady state frequency without AGC is dropped to 49.64 Hz which is out of normal control. To keep the frequency back in the control range, the AGC has to control all conventional online-generators and produce more power to compensate the decrease of solar power which requires 13 second for this response.

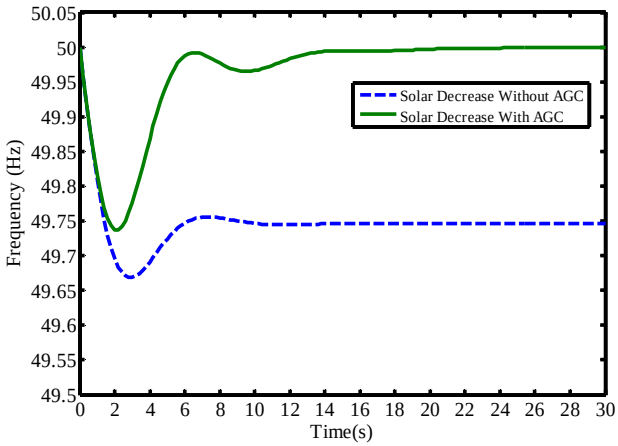

Fig. 9. Frequency response of PL with and without AGC.

Frequency Response for Next Two Decades

For the next two decades, the maximum frequency deviations of Thailand's power system have probably incremental trends due to influence of incremental solar power capacity as shows in Figure 10. In addition, the simulation results show that the highest frequency deviations can be observed at the PPL which presented larger step change of solar power and load while the number of online-generators for reserve power is less than PL condition. In case of LL condition, maximum frequency deviations are stayed in normal control range ($\pm$0.1 Hz) during years 2014-2022 after those similar maximum frequency deviations are out of normal control range. In cases of PPL and PL, all of the maximum frequency deviations of years 2014-2030 are out of normal control range. Moreover, comparison between year 2014 and year 2030, the maximum frequency deviation is increased 0.22 Hz as a results of increasing solar power capacity by 3,080 MW. However, this result is not considered the diversity of solar power outputs in the different locations.

The increasing of solar power plants will lead the frequency response of Thailand's power system to the weakest system because the total inertia of the system is reduced by the ratio of total solar power plants with total power plants. However the Thailand's power system can maintain system reliability and security for sustainable power development plan with solar power plants by realizing the ratio of total solar power plants with total power plants but impossible for realistic PDP. The further study of solar power plant controller especially modern inverter is needed to handle the fluctuation of solar radiation for frequency deviation. Finally, the additional regulation for solar power plants in term of energy storage requirement will be studied to optimize between incremental cost of energy storage and the system stability.

6. CONCLUSION

This paper presents frequency responses of Thailand's power system for the next two decades by considering influences of solar power integrations according to the PDP 2010 version 3. The developed RIPT frequency response model which is time dependent model based on

characteristics of online-generators at specific time, is used to investigate impacts of solar power deviation. The simulations are performed through multi-scenarios of power plant operating condition, the light load (LL), the partial peaked load (PPL) and the peaked load (PL) with the assumptions of maximum solar power deviations. The results present the frequency responses of each operating conditions for 16 years of the PDP. In addition, the results show that maximum frequency deviations of Thailand's power system have probably incremental trends due to influence of incremental solar power capacities. The highest frequency deviation is 0.377 Hz which can be observed in PPL operating condition in the year 2030 with the 3,940 MW installed capacity of solar power plant.

Actually, these impacts of solar power deviation can be solved by application of various energy storages. Finally, the further studies in more details about long term planning of solar power plant for frequency response are very important to maintain reliability of the power system in critical period as well as PPL, system operators have to provide reserve power to ensure that there is enough governing and load response to keep the frequency in the normal control range. However, long term protective planning is needed as well as the regulation for solar power plants.

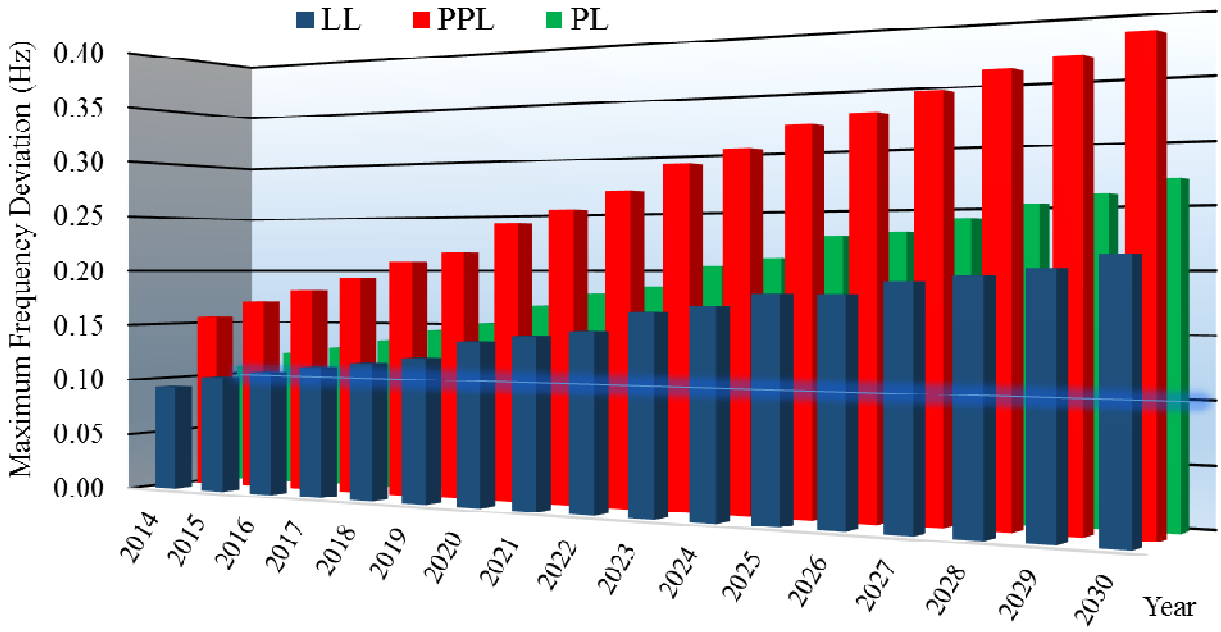

Fig. 10. Simulation results of maximum frequency deviations divided by operating condition through 20 years of PDP 2010.

ACKNOWLEDGEMENT

This research was supported by EGAT–NSTDA Research and Development Promotion Fund.

REFERENCES

[1] Energy Policy and Planning Office, Ministry of Energy, Thailand (2014). Power Development Plan 2010 Revision 3.

[2] Department of Alternative Energy Development and Efficiency 2012. The Renewable and Alternative Energy Development Plan for 25 Percent in 10 Years (AEDP 2012-2021).

[3] BP Statistical Review of World Energy 2014. [On-line] Avalible on: http://www.bp.com/content/dam /bp/pdf/ Energy- economics/statistical-review-2014 [Oct 10, 2014].

[4] Kunpur P. 1991. Power system stability and control, McGraw-Hill, Englewood Cliffs, NJ.

[5] Saadat, H. 1999. Power System Analysis. McGraw-Hill.

[6] Gillian L., Julia R., Damian F. and Mark J. O'Malley 2005. Power Systems: The Impact of Combined-Cycle Gas Turbine Short-Term Dynamics on Frequency Control, vol. 20, No. 3, pp. 1456-1464.

[7] Bevrani H. 2009. Robust power system frequency control. Springer, New York.

[8] Lisa R., Nicholas W. Jonathan O and Damian F. 2012. Sustainable Energy. Frequency Response of Power Systems with Variable Speed Wind Turbines, vol. 3, no. 4, pp. 683-691.

[9] Bevrani H., Ghosh A. and Ledwich G. 2010. Renewable energy sources and frequency regulation: survey and new perspectives. *IET Renewable Power Generation*.

[10] Sandip S, Shun H. H. and NDR Sarma. System Inertial Frequency Response Estimation and Impact of Renewable Resources in ERCOT Interconnection, Electric Reliability Council of Texas (ERCOT, Inc), USA.

One Rank Cuckoo Search Algorithm for Optimal Reactive Power Dispatch

Nguyen Huu Thien An, Vo Ngoc Dieu, Thang Trung Nguyen and Vo Trung Kien

Abstract— *This paper proposes a one rank cuckoo search algorithm (ORCSA) for solving optimal reactive power dispatch (ORPD) problem. The proposed ORCSA can deal with different objectives of the problem such as minimizing the real power losses, improving the voltage profile, and enhancing the voltage stability and properly handle various constraints for reactive power limits of generators and switchable capacitor banks, bus voltage limits, tap changer limits for transformers, and transmission line limits. The ORCSA method is created based on the conventional CSA method so as to improve optimal solution and speed up convergence. In the ORCSA method, new eggs generated via Lévy flights are replaced partially and the newly generated eggs are then evaluated and ranked at once. On the other hand, there is a bound by best solution technique proposed for replacing the invalid dimension in order to improve convergence rate and performance. The proposed method has been tested on the IEEE 30-bus and IEEE 118- bus systems and the obtained results are compared to that from other methods reported in the paper has indicated that the proposed method is very efficient for the optimal reactive power optimization problems.*

***Keywords*— Constriction factor, optimal reactive power dispatch, one rank cuckoo search algorithm, voltage deviation, voltage stability index.**

1. INTRODUCTION

Optimal reactive power dispatch (ORPD) is to determine the control variables such as generator voltage magnitudes, switchable VAR compensators, and transformer tap setting so that the objective function of the problem is minimized while satisfying the unit and system constraints [1]. In the ORPD problem, the objective can be total power loss, voltage deviation at load buses for voltage profile improvement [2], or voltage stability index for voltage stability enhancement [3]. ORPD is a complex and large-scale optimization problem with nonlinear objective and constraints. In power system operation, the major role of ORPD is to maintain the load bus voltages within their limits for providing high quality of services to consumers.

The problem has been solved by various techniques ranging from conventional methods to artificial intelligence based methods. Several conventional methods have been applied for solving the problem such as linear programming (LP) [4], [1]mixed integer programming (MIP) [5], interior point method (IPM) [6], dynamic programming (DP) [7], and quadratic programming (QP) [8]. These methods are based on successive linearizations and use gradient as search directions. The conventional optimization methods can properly deal with the optimization problems of deterministic quadratic objective function and differential constraints. However, they can be trapped in local minima of the ORPD problem with multiple minima [9]. Recently, meta-heuristic search methods have become popular for solving the ORPD problem due to their advantages of simple implementation and ability to find near optimum solution for complex optimization problems. Various meta-heuristic methods have been applied for solving the Problem such as evolutionary programming (EP) [9], genetic algorithm (GA) [3], ant colony optimization algorithm (ACOA) [10], differential evolution (DE) [11], harmony search (HS) [12], etc. These methods can improve optimal solutions for the ORPD problem compared to the conventional methods but with relatively slow performance.

In this paper, a One Rank Cuckoo Search Algorithm (ORCSA) [13] is first proposed for the ORPD problem. The ORCSA is developed by Ahmed et al in 2013 by performing two modifications on original Cuckoo Search Algorithm including merging exploration phase and exploitation phase and bound by best solution mechanism.

In this paper, the proposed method has been tested on the IEEE 30-bus and IEEE 118-bus systems and the obtained results are compared to those from Particle Swarm Optimizer (PSO), Self-Organizing Hierarchical Particle Swarm Optimizer - Time Varying Acceleration Coefficients (HPSO-TVAC), Particle Swarm Optimization - Time Varying Acceleration Coefficients (PSO-TVAC), and Firefly Algorithm (FA). The result comparison has shown that the proposed method can obtain total power loss, voltage deviation or voltage stability index less than the others for the considered cases. Therefore, the proposed CRCSA can be a

Nguyen Huu Thien An (corresponding author), Vo Ngoc Dieu, and Vo Trung Kien are with Ho Chi Minh City University of Technology, Ho Chi Minh City, Vietnam. Email: annht.bk@gmail.com.

Thang Trung Nguyen is with Electrical and Electronics Engineering University of Technical Education Ho Chi Minh City, Ho Chi Minh city, Vietnam.

favorable method for implementation in the optimal reactive power optimization problems.

2. PROBLEM FORMULATION

The objective of the ORPD problem is to minimize is to optimize the objective functions while satisfying several equality and inequality constraints.

Mathematically, the problem is formulated as follows:

$$MinF(x,u) \tag{1}$$

where the objective function *F(x,u)* can be expressed in one of the forms as follows:

- Real power loss:

$$F(x,u) = P_{loss} = \sum_{i=1}^{N_l} g_l \begin{bmatrix} V_i^{\,2} + V_j^{\,2} \\ -2V_i V_j \cos(\delta_i - \delta_j) \end{bmatrix} \tag{2}$$

- Voltage deviation at load buses for voltage profile improvement [2]:

$$F(x,u) = VD = \sum_{i=1}^{N_d} \left| V_i - V_i^{sp} \right| \tag{3}$$

where V_i^{sp} is the pre-specified reference value at load bus *i*, which is usually set to 1.0 pu.

- Voltage stability index for voltage stability enhancement [3], [18]:

$$F(x,u) = L_{\max} = \max\{L_i\}; i = 1,..., N_d \tag{4}$$

For all the considered objective functions, the vector of dependent variables *x* represented by:

$$x = [Q_{gl},..., Q_{gN_g}, V_{l1},..., V_{lN_d}, S_1,..., S_{N_l}]^T \tag{5}$$

and the vector of control variables *u* represented by:

$$u = [V_{gl},..., V_{gN_g}, T_1,..., T_{N_t}, Q_{c1},..., Q_{cN_c}]^T \tag{6}$$

The problem includes the equality and inequality constraints as follows:

a) Real and reactive power flow equations at each bus:

$$P_{gi} - P_{di} = V_i \sum_{j=1}^{N_b} V_j \left[G_{ij} \cos(\delta_i - \delta_j) + B_{ij} \sin(\delta_i - \delta_j) \right] \tag{7}$$

$i = 1,..., N_b$

$$Q_{gi} - Q_{di} = V_i \sum_{j=1}^{N_b} V_j \left[G_{ij} \sin(\delta_i - \delta_j) - B_{ij} \cos(\delta_i - \delta_j) \right] \tag{8}$$

$i = 1,..., N_b$

b) Voltage and reactive power limits at generation buses:

$$V_{gi,\min} \le V_{gi} \le V_{gi,\max}; i = 1,..., N_g \tag{9}$$

$$Q_{gi,\min} \le Q_{gi} \le Q_{gi,\max}; i = 1,..., N_g \tag{10}$$

c) Capacity limits for switchable shunt capacitor banks:

$$Q_{ci,\min} \le Q_{ci} \le Q_{ci,\max}; i = 1,..., N_c \tag{11}$$

d) Transformer tap settings constraint:

$$T_{k,\min} \le T_k \le T_{k,\max}; k = 1,..., N_t \tag{12}$$

e) Security constraints for voltages at load buses and transmission lines:

$$V_{li,\min} \le V_{li} \le V_{li,\max}; i = 1,..., N_d \tag{13}$$

$$S_l \le S_{l,\max}; l = 1,..., N_l \tag{14}$$

where the S_l is the maximum power flow between bus *i* and bus *j* determined as follows:

$$S_l = \max\left\{ |S_{ij}|, |S_{ji}| \right\} \tag{15}$$

3. ONE RANK CUCKOO SEARCH ALGORITHM (ORCSA)

3.1. One Rank Cuckoo Search Algorithm (ORCSA):

The cuckoo search algorithm (CSA), a new meta-heuristic algorithm, is inspired from the obligate brood parasitism of some cuckoo species by laying their eggs in the nests of other host birds of other species for solving optimization problems. The CSA was first developed by was first developed by Yang and Deb in 2009. The CSA is summarized in the three main principal rules as follows [15]:

1. A cuckoo bird lays an egg and chooses a nest among the predetermined number of available host nests to dump its egg.

2. The best nests with high quality of egg (better solution) will be carried over to the next generation.

3. The number of available host nests is fixed, and the egg laid by a cuckoo is discovered by the host bird with a probability probability pa∈ [0, 1]. For the fraction of eggs, the host bird can either throw them away, or abandon them and build a new nest.

There is one more parameter is introduced in the proposed method in order to decide if the computational process merges exploration phase and exploitation phase together, called one rank ratio ror. The task of selection of the ratio is easy. It is initially set to 1 to allow merging new eggs from exploration phase and exploitation phase together. The ratio is still fixed at 1 until a better nest cannot be found at a current iteration. For the situation, the ratio is reduced as in the following equation (16).

$$r_{or}^{Iter+1} = r_{or}^{Iter} - 0.5 / D \tag{16}$$

where Iter is the current iteration and D is the number of objective function dimension.

On the other hand, there is a bound by best solution technique proposed for replacing the invalid dimension in order to improve convergence rate and performance.

$$r_{bbb} = 1 - 1/\sqrt{D} \tag{17}$$

3.2. ORCSA for the ORPD problem

3.2.1. Initialization

For implementation of the proposed ORCSA to the

problem, control variables is defined as follows:

$$x_d = [V_{g1d},...,V_{gN_g d},T_{1d},...,T_{N_t d},Q_{c1d},...,Q_{cN_c d}]^T \quad d = 1,...,N \tag{18}$$

Initialize input of X_{id} is determined:

$$X_{id} = X_{id}^{\min} + rand(N,FS).*\left(X_{id}^{\max} - X_{id}^{\min}\right) \tag{19}$$

In which

$$X_{id}^{\max} = X_i^{\max} * ones(1,FS) \tag{20}$$

$$X_{id}^{\min} = X_i^{\min} * ones(1,FS) \tag{21}$$

with

$$X_{id}^{\max} = [V_{g1d}^{\max},...,V_{gN_g d}^{\max},T_{1d}^{\max},...,T_{N_t d}^{\max},Q_{c1d}^{\max},...,Q_{cN_c d}^{\max}] \tag{22}$$

$$X_{id}^{\min} = [V_{g1d}^{\min},...,V_{gN_g d}^{\min},T_{1d}^{\min},...,T_{N_t d}^{\min},Q_{c1d}^{\min},...,Q_{cN_c d}^{\min}] \tag{23}$$

The fitness function to be minimized is based on the problem objective function and dependent variables including reactive power generations, load bus voltages, and power flow in transmission lines. The fitness function is defined as follows:

$$F_T = F(x,u) + K_q\sum_{i=1}^{N_g}(Q_{gi} - Q_{gi}^{\lim})^2 + K_v\sum_{i=1}^{Nd}(V_{li} - V_{li}^{\lim})^2 + K_s\sum_{l=1}^{N_l}(S_l - S_{lmax})^2 \tag{24}$$

where K_q, K_v and K_s are penalty factor for reactive power generations, load bus voltages, and power flow in transmission lines, respectively.

The limits of the dependent variables in (24) are determined based on their calculated values as follows:

$$x^{\lim} = \begin{cases} x_{\max} & x > x_{\max} \\ x_{\min} & x < x_{\min} \end{cases} \tag{25}$$

whrere x and x^{lim} respectively represent for the calculated value and limits of Q_{gi}, V_{li}, S_{lmax}.

3.2.2. Generation of New Solution via Lévy Flights

The new solution is calculated based on the previous best nests via Lévy flights. In the proposed CSA method, the optimal path for the Lévy flights is calculated by Mantegna's algorithm (Mantegna,1994) [16]. The new solution by each nest is calculated as follows:

$$X_d^{new} = Xbest_d + \alpha \times rand_3 \times \Delta X_d^{new} \tag{26}$$

where $\alpha > 0$ is the updated step size; $rand_3$ is a normally distributed random number in [0, 1] and the increased value ΔX_d^{new} is determined by:

$$\Delta X_d^{new} = v \times \frac{\sigma_x(\beta)}{\sigma_y(\beta)} \times (Xbest_d - Gbest) \tag{27}$$

where

$$v = \frac{rand_x}{\left|rand_y\right|^{1/\beta}} \tag{28}$$

where randx and randy are two normally distributed stochastic variables with standard deviation $\sigma x(\beta)$ and $\sigma y(\beta)$ given by:

$$\sigma_x(\beta) = \left[\frac{\Gamma(1+\beta)\times\sin\left(\frac{\pi\beta}{2}\right)}{\Gamma\left(\frac{1+\beta}{2}\right)\times\beta\times 2^{\left(\frac{\beta-1}{2}\right)}}\right]^{1/\beta} \tag{29}$$

$$\sigma_y(\beta) = 1 \tag{30}$$

where β is the distribution factor ($0.3 \le \beta \le 1.99$) and $\Gamma(.)$ is the gamma distribution function.

3.2.3. Alien Egg Discovery and Randomization

The action of discovery of an alien egg in a nest of a host bird with the probability of pa also creates a new solution for the problem similar to the Lévy flights. The new solution due to this action can be found out in the following way:

$$X_d^{dis} = Xbest_d + K \times \Delta X_d^{dis} \tag{31}$$

where $Xbest_d$ is a solution generated via Lévy flights as in section 3.2.2 and K is the updated coefficient determined based on the probability of a host bird to discover an alien egg in its nest:

$$K = \begin{cases} 1 & \text{if } rand_4 < p_a \\ 0 & \text{otherwise} \end{cases} \tag{32}$$

and the increased value ΔX_d^{dis} is determined by:

$$\Delta X_d^{dis} = rand_5 \times [randp_1(Xbest_d) - randp_2(Xbest_d)] \tag{33}$$

where $rand_4$ and $rand_5$ are the distributed random numbers in [0, 1] and $randp1(Xbest_d)$ and $randp2(Xbest_d)$ are the random perturbation for positions of the nests in $Xbest_d$.

3.2.4. Bound by best solution mechanism

For the newly obtained solution using Matpower toolbox 4.1, its upper and lower limits should be satisfied. As described in the second modification in section 3.1, the bound by best solution mechanism is used to handle the inequality constraint.

3.2.5. Stopping Criteria

The algorithm is stopped when the number of iterations (Iter) reaches the maximum number of iterations (Itermax).

The overall procedure of the proposed ORCSA for solving the ORPD problem is addressed as follows:

Step 1: Select parameters for ORCSA including the number of nest Np, the maximum number of iteration Itermax. Initialize population of host nests as in Section 3.2.1.

Step 2: Calculate value of dependent variables based on power flow solution using Matpower

toolbox 4.1.

Step 3: Evaluate fitness function to choose Xbest and Gbest based on the value of their fitness function. Set the iteration counter *Iter* = 1 and one rank ratio r_{or} = 1.

Step 4: Set Generate new solutions for abandoned eggs via Lévy flights as in Section 3.2.2

Step 5: Initialize a random number and compare to one rank ratio r_{or}. If the random number is less than r_{or}, go to step 6. Otherwise, go to step 9

Step 6: Discover alien egg and randomize to generate new solution as in Section 3.2.3

Step 7: Perform bound by best solution mechanism to define new solution as in section 3.2.4.

Step 8: Calculate value of dependent variables based on power flow solution using Matpower toolbox 4.1. Calculate fitness function (24), then rank and keep the current best nest. Go to step 14.

Step 9: Perform bound by best solution mechanism to define new solution as in section 3.2.4.

Step 10: Calculate value of dependent variables based on power flow solution using Matpower toolbox 4.1. Calculate fitness function (24), then rank and keep the current best nest.

Step 11: Discover alien egg and randomize to generate new solution as in Section 3.2.3

Step 12: Perform bound by best solution mechanism to define new solution as in section 3.2.4.

Step 13: Calculate value of dependent variables based on power flow solution using Matpower toolbox 4.1. Calculate fitness function (24), then rank and keep the current best nest.

Step 14: Get the best nest Gbest.

Step 15: If the current iteration Iter is equal to the maximum number of predetermined iteration. Stop the iterative procedure. Otherwise, set *Iter* = *Iter* + 1 and go to step 16.

Step 16: If the best nest Gbest at the current iteration is not better than that of the previous iteration. Obtain the one rank ratio using eq. (16) and back to 5.

4. NUMERICAL RESULTS

The proposed ORCSA has been tested on the IEEE 30-bus and 118-bus systems with different objectives including power loss, voltage deviation, and voltage stability index. The data for these systems can be found in [19], [20] . The characteristics and the data for the base case of the test systems are given in Tables 1 and 2, respectively.

The algorithms of the ORCSA methods are coded in Matlab R2009b and run on an Intel Core i3 CPU 2.50 GHz with 2 GB of RAM PC. The parameters of the ORCSA methods for the test systems are summarized in Table 3.

4.1 IEEE 30-bus system:

In the test system, the generators are located at buses 1, 2, 5, 8, 11, and 13 and the available transformers are located on lines 6-9, 6-10, 4-12, and 27-28. The switchable capacitor banks will be installed at buses 10, 12, 15, 17, 20, 21, 23, 24, and 29 with the minimum and maximum values of 0 and 5 MVAR, respectively. The limits for control variables are given in [11], generation reactive power in [21], and power flow in transmission lines in [22].

The results obtained by the ORCSA method for the system with different objectives including power loss, voltage deviation for voltage profile improvement, and voltage stability index for voltage enhancement are given in Tables 4, 5, and 6, respectively and the solutions for best results are given in Tables A1, A2, and A3 of Appendix.

The obtained best results from the proposed ORCSA method are compared to Gravitational Search Algorithm (GSA), comprehensive learning particle swarm optimization (CLPSO) [23], Self-Organizing Hierarchical Particle Swarm Optimizer - Time Varying Acceleration Coefficients (HPSO-TVAC), Particle Swarm Optimization - Time Varying Acceleration Coefficients (PSO-TVAC) [24] and Firefly Algorithm (FA) [25] for different objectives as given in Table 7.

The obtained best results from the proposed ORCSA method are compared to those from DE [11], comprehensive learning particle swarm optimization (CLPSO) [23], PSO variants [24], and FA [25] for different objectives as given in Table 7. For the objective of total power loss and voltage deviation, the optimal solutions by the proposed ORCSA are less than those from the others while the best voltage stability index from the ORCSA method is approximate to that from others. For computational time, the ORCSA method obtained its optimal solution for an average of 15 seconds which is similar that from the PSO-CF method. For computational time, the ORCSA method obtained its optimal solution for an average of 15 seconds which is similar that from the other methods.

Table 1. Characteristics of test systems

System	No. of branches	No. of Generatio buses	No. of transformers	No. of capacitor banks	No. of control variables
IEEE 30 bus	41	6	4	9	19
IEEE 118 bus	186	54	9	14	77

Table 2. Base case for test systems

System	$\sum P_{di}$	$\sum Q_{di}$	$\sum P_{gi}$	$\sum Q_{gi}$
IEEE 30 bus	283.4	126.2	287.92	89.2
IEEE 118 bus	4242	1438	4374.86	795.68

Table 3: The parameters of the ORCSA methods

	Number of nest	Pa	Alpha1
ORCS algorithm	10	0.7	0.1

Table 4. Results by ORCSA method and compare to the other methods for the IEEE 30-bus system with power loss objective

Method	PSO-TVAC [24]	HPSO-TVAC [24]	ORCS
Min Ploss (MW)	4.5356	4.5283	4.5134
Avg. Ploss (MW)	4.5912	4.5581	4.5873
Max Ploss (MW)	4.9439	4.6112	5.1346
Std. dev. Ploss (MW)	0.0592	0.0188	0.1181
VD	1.9854	1.9315	2.0460
L_{max}	0.1257	0.1269	0.1256
Avg. CPU time (s)	10.38	10.65	14.719

Table 5. Results by ORCSA method and compare to the other methods for the IEEE 30-bus system with voltage deviation objective

Method	PSO-TVAC [24]	HPSO-TVAC [24]	ORCS
Min VD	0.1210	0.1136	0.0946
Avg. VD	0.1529	0.1340	0.1041
Max VD	0.1871	0.1615	0.1229
Std. dev. VD	0.0153	0.0103	0.0049
Ploss (MW)	5.3829	5.7269	5.6809
Slmax	0.1485	0.1484	0.1478
Avg. CPU time (s)	9.88	9.59	15.622

Table 6. Results by ORCSA method and compare to the other methods for the IEEE 30-bus system with voltage stability index objective

Method	PSO-TVAC [24]	HPSO-TVAC [24]	ORCS
Min Lmax	0.1248	0.1261	0.1249
Avg. Lmax	0.1262	0.1275	0.1258
Max Lmax	0.1293	0.1287	0.1269
Std. dev. Lmax	0.0009	0.0006	0.0004
Ploss (MW)	4.8599	5.2558	4.6584
VD	1.9174	1.6830	1.9975
Avg. CPU time (s)	13.39	13.05	15.150

Table 7. Comparison of best results for the IEEE 30-bus system

Method / Function	Power loss (MW)	Voltage deviation (VD)	Stability index (L_{imax})
CLPSO[23]	4.5615	-	-
PSO-TVAC[24]	4.5356	0.1210	0.1248
HPSO-TVAC[24]	4.5283	0.1136	0.1261
HFA [25]	4.529	0.098	-
ORCSA	4.5134	0.0946	0.1247

Table 8. Results by ORCSA method and compare to the other methods for the IEEE 118-bus system with power loss objective

Method	PSO-TVAC [24]	HPSO-TVAC [24]	ORCS
Min Ploss (MW)	124.3335	116.2026	116.9774
Avg. Ploss (MW)	129.7494	117.3553	122.1781
Max Ploss (MW)	134.1254	118.1390	122.1781
Std. dev. Ploss (MW)	2.1560	0.4696	2.4681
VD	1.4332	1.8587	2.0636
Lmax	0.0679	0.0650	0.0632
Avg. CPU time (s)	85.32	85.25	104.062

Table 9. Results by ORCSA methods and compare to the other methods for the IEEE 118-bus system with voltage deviation objective

Method	PSO-TVAC [24]	HPSO-TVAC [24]	ORCS
Min VD	0.3921	0.2074	0.3101
Avg. VD	0.4724	0.2498	0.4345
Max VD	0.5407	0.3012	0.5827
Std. dev. VD	0.0316	0.0215	0.0596
Ploss (MW)	179.7952	146.8104	136.0782
Slmax	0.0667	0.0670	0.0672
Avg. CPU time (s)	78.70	74.90	137.640

Table 10. Results by ORCSA methods and compare to the other methods for the IEEE 118-bus system with stability index objective

Method	PSO-TVAC [24]	HPSO-TVAC [24]	ORCS
Min Lmax	0.0607	0.0607	0.0595
Avg. Lma	0.0609	0.0608	0.0633
Max Lmax	0.0613	0.0612	0.0712
Std. dev. Lmax	0.0001	0.0001	0.0023
Ploss (MW)	184.5627	155.3915	131.9501
VD	1.2103	1.34401	1.3862
Avg. CPU time (s)	119.22	119.16	137.316

Table 11. Comparison of best results for the IEEE 118-bus system

Method / Function	Power loss (MW)	Voltage deviation (VD)	Stability index (L_{imax})
PSO-TVAC[24]	124.3335	0.3921	0.0607
PSO[24]	131.99	2.2359	0.1388
CLPSO[15]	130.96	1.6177	0.0965
FA [25]	135.42	0.378	-
ORCSA	116.9774	0.3101	0.0595

4.2 IEEE 118-bus system

In this system, the position and lower and upper limits for switchable capacitor banks, and lower and upper limits of control variables are given in [23].

The obtained results by the ORCSA methods for the system with different objectives similar to the case of IEEE 30 bus system are given in Tables 8, 9, and 10, respectively and the comparison of best results from methods for different objectives is given in Table 11. It can be seen from the data in Table 11 that the results obtained from the ORCSA method are less than others methods with total power loss, voltage deviation, and voltage stability index. For computational time, the ORCSA method obtained its optimal solution for an average of 137 seconds which is similar that from the other methods.

5. CONCLUSION

In this paper, the ORCSA method has been effectively and efficiently implemented for solving the ORPD problem. The proposed ORCSA has been tested on the

IEEE 30-bus and IEEE 118-bus systems with different objectives including power loss, voltage deviation, and voltage stability index. The test results have shown that proposed method can obtain total power loss, voltage deviation, or voltage stability index less than other methods for test cases. Therefore, the proposed ORCSA could be a useful and powerful method for solving the ORPD problem.

REFERENCES

[1] Nanda, J., Hari, L. and Kothari, M. L. 1992, Challenging algorithm for optimal reactive power dispatch through classical co-ordination equations", *IEE Proceedings - C*, vol. 139, no. 2, pp. 93-101.

[2] Vlachogiannis, J. G. and Lee, K. Y. 2006. A Comparative study on particle swarm optimization for optimal steady-state performance of power systems. *IEEE Trans. Power Systems*, vol. 21, no. 4, pp. 1718-1728.

[3] Devaraj, D. and Preetha Roselyn, J. 2010. Genetic algorithm based reactive power dispatch for voltage stability improvement. *Electrical Power and Energy Systems*, vol. 32, no. 10, pp. 1151-1156.

[4] Kirschen, D. S. and Van Meeteren H. P. 1988. MW/voltage control in a linear programming based optimal power flow. *IEEE Trans. Power Systems*, vol. 3, no. 2, pp. 481-489.

[5] Aoki, K., Fan, M. and Nishikori, A. 1988. Optimal VAR planning by approximation method for recursive mixed integer linear programming. *IEEE Trans. Power Systems*, vol. 3, no. 4, pp. 1741-1747.

[6] Granville, S. 1994. Optimal reactive power dispatch through interior point methods. *IEEE Trans. Power Systems*, vol. 9, no. 1, pp. 136-146.

[7] Lu, F. C. and Hsu, Y. Y. 1994. Reactive power/voltage control in a distribution substation using dynamic programming. *IEE Proc. Gen. Transm. Distrib.*, vol. 142, no. 6, pp. 639–645.

[8] Grudinin, N. 1998. Reactive power optimization using successive quadratic programming method. *IEEE Trans. Power Systems*, vol. 13, no. 4, pp.1219-1225.

[9] Lai, L. L. and Ma, J. T. 1997. Application of evolutionary programming to reactive power planning - Comparison with nonlinear programming approach. *IEEE Trans. Power Systems*, vol. 12, no. 1, pp. 198-206.

[10] Abou El-Ela, A., Kinawy, A., El-Sehiemy, R. and Mouwafi, M. 2011. Optimal reactive power dispatch using ant colony optimization algorithm. *Electrical Engineering (Archiv fur Elektrotechnik)*, pp. 1-14. Retrieved Feb. 20, 2011, from http://www.springerlink.com/ content/k02v360632653864.

[11] Abou El Ela, A. A., Abido, M. A. and Spea, S. R. 2011. Differential evolution algorithm for optimal reactive power dispatch. *Electric Power Systems Research*, vol. 81, no. 2, pp. 458- 464.

[12] Khazali, A. H. and Kalantar, M. 2011. Optimal reactive power dispatch based on harmony search algorithm. *Electrical Power and Energy Systems*, vol. 33, no. 3, pp. 684-692.

[13] Ahmed, S. T., Amr, A.B. & Ibrahim, F. A. (2013). One Rank Cuckoo Search Algorithm with Application to Algorithmic, Trading Systems Optimization. *International Journal of Computer Applications*, vol. 64, no. 6, pp. 30-37.

[14] Yang, X.S. & Deb, S. (2009). Cuckoo search via Lévy flights. In *Proc. World Congress on Nature & Biologically Inspired Computing (NaBIC 2009)*, India, p. 210-214.

[15] Xiangtao, L. & Minghao, Y. (2013). A hybrid cuckoo search via Lévy flights for the permutation flow shop scheduling problem. Int. J. Prod Res, 51, pp. 4732-54.

[16] Mantegna, R.N. (1994). Fast, accurate algorithm for numerical simulation of Levy stable stochastic processes. *Phys Rev E.*, vol. 49, pp. 4677-4683.

[17] Walton, S., Hassan, O., Morgan, K. & Brown, M.R. (2011). Modified cuckoo search: A new gradient free optimisation algorithm. *Chaos, Solutions & Fractals*, vol. 44, pp. 710–718.

[18] Kessel, P. and Glavitsch, H. 1986. Estimating the voltage stability of power systems. *IEEE Trans Power Systems*, vol. 1, no. 3, pp. 346–54.

[19] Dabbagchi, I. and Christie, R. 2011. Power systems test case archive. Retrieved Feb. 20, 2011, from http://www.ee.washington.edu/ research/pstca/.

[20] Zimmerman, R. D., Murillo-Sánchez, C. E. and Thomas, R. J. 2009. Matpower's extensible optimal power flow architecture. In *Proc. Power and Energy Society General Meeting*, pp. 1-7.

[21] Lee, K. Y., Park, Y. M. and Ortiz, J. L. 1985. A united approach to optimal real and reactive power dispatch. *IEEE Trans. Power Apparatus and Systems*, vol. PAS-104, no. 5, pp. 1147-1153.

[22] Alsac, O. and Stott, B. 1974. Optimal load flow with steady-state security. *IEEE Trans. Power Apparatus and Systems*, vol. 93, pp. 745-751.

[23] Mahadevan, K. and Kannan, P. S. 2010. Comprehensive learning particle swarm optimization for reactive power dispatch. *Applied Soft Computing*, vol. 10, no. 2, pp. 641-652.

[24] Vo Ngoc Dieu and Peter Schegner, 2011. Particle swarm optimization with constriction factor for optimal reactive power dispatch. In *Proceedings of the fifth Global Conference on Power Control and Optimization (PCO)*, 1-3 June, 2011, Dubai, Unites Arab Emirate.

[25] Abhishek Rajan, T. Malakar, 2015. Optimal reactive power dispatch using hybrid Nelder–Mead simplex based firefly algorith. *Electrical Power and Energy Systems*, vol. 66, pp. 9–24.

APPENDIX

The best solutions by ABC methods for the IEEE 30- bus system with different objectives are given in Tables A1, A2, and A3.

Table A1. Best solutions by ORCSA methods for the IEEE 30-bus system with power loss objective

Control variables	PSO-TVAC	HPSO-TVAC	HFA	ORCSA
V_{g1}	1.1000	1.1000	1.1	1.1000
V_{g2}	1.0957	1.0941	1.054332	1.0937
V_{g5}	1.0775	1.0745	1.075146	1.0734
V_{g8}	1.0792	1.0762	1.086885	1.0756
V_{g11}	1.1000	1.0996	1.1	1.0997
V_{g13}	1.0970	1.1000	1.1	1.1000
$T_{6\text{-}9}$	1.0199	1.0020	0.980051	1.0374
$T_{6\text{-}10}$	0.9401	0.9498	0.950021	0.9058
$T_{4\text{-}12}$	0.9764	0.9830	0.970171	0.9782
$T_{27\text{-}28}$	0.9643	0.9707	0.970039	0.9648
Q_{c10}	4.5982	2.3238	4.700304	4.9985
Q_{c12}	2.8184	2.8418	4.706143	4.7287
Q_{c15}	2.3724	3.6965	4.700662	4.3016
Q_{c17}	3.6676	4.9993	2.30591	4.8615
Q_{c20}	4.3809	3.1123	4.80352	4.2635
Q_{c21}	4.9146	4.9985	4.902598	4.9711
Q_{c23}	3.6527	3.5215	4.804034	2.9871
Q_{c24}	5.0000	4.9987	4.805296	4.9866
Q_{c29}	2.1226	2.3743	3.398351	2.2062

Table A2. Best solutions by ORCSA methods for the IEEE 30-bus system with voltage deviation objective

Control variables	PSO-TVAC	HPSO-TVAC	HFA	ORCSA
V_{g1}	1.0282	1.0117	1.003458	1.0169
V_{g2}	1.0256	1.0083	1.01638	1.0148
V_{g5}	1.0077	1.0169	1.019451	1.0175
V_{g8}	1.0014	1.0071	1.018221	1.0115
V_{g11}	1.0021	1.0707	0.982272	1.0157
V_{g13}	1.0046	1.0060	1.01546	0.9931
$T_{6\text{-}9}$	1.0125	1.0564	0.99	1.0314
$T_{6\text{-}10}$	0.9118	0.9076	0.9	0.9002
$T_{4\text{-}12}$	0.9617	0.9545	0.98	0.9513
$T_{27\text{-}28}$	0.9663	0.9695	0.96	0.9576
Q_{c10}	5.0000	1.5543	3.2	4.0287
Q_{c12}	1.5065	1.4242	0.5	3.0711
Q_{c15}	3.9931	2.5205	4.9	4.2692
Q_{c17}	3.7785	1.6400	0.1	0.9329
Q_{c20}	3.2593	5.0000	3.8	4.9825
Q_{c21}	4.1425	1.8539	5	2.6228
Q_{c23}	4.9820	3.3035	5	4.9425
Q_{c24}	4.5450	4.5941	3.9	4.7014
Q_{c29}	4.1272	3.5062	1.5	2.3272

Table A3. Best solutions by ORCSA methods for the IEEE 30-bus system with objective of stability index

Thông số biến	PSO-TVAC	HPSO-TVAC	ORCSA
V_{g1}	1.1000	1.0979	1.0996
V_{g2}	1.0934	1.0997	1.0949
V_{g5}	1.0969	1.0500	1.0791
V_{g8}	1.0970	1.0663	1.0723
V_{g11}	1.1000	1.0561	1.0975
V_{g13}	1.1000	1.0886	1.0958
$T_{6\text{-}9}$	1.0935	0.9939	0.9693
$T_{6\text{-}10}$	0.9000	1.0150	0.9068
$T_{4\text{-}12}$	0.9579	0.9121	0.9815
$T_{27\text{-}28}$	0.9651	0.9406	0.9458
Q_{c10}	3.1409	3.7685	3.2972
Q_{c12}	3.0186	4.6323	2.2557
Q_{c15}	1.4347	2.6542	4.6097
Q_{c17}	3.8498	2.6897	0.5020
Q_{c20}	0.0000	2.8806	1.8554
Q_{c21}	5.0000	2.1071	1.1608
Q_{c23}	0.0000	3.1044	0.8344
Q_{c24}	2.1733	2.1797	0.3412
Q_{c29}	2.2708	3.5843	3.9241

GMSARN International Journal
NOTES FOR AUTHORS

Editorial Policy

In the Greater Mekong Subregion, home to about 250 million people, environmental degradation - including the decline of natural resources and ecosystems will definitely impact on the marginalized groups in society - the poor, the border communities especially women and children and indigenous peoples. The complexity of the challenges are revealed in the current trends in land and forest degradation and desertification, the numerous demands made on the Mekong river - to provide water for industrial and agricultural development, to sustain subsistence fishing, for transport, to maintain delicate ecological and hydrological balance, etc., the widespread loss of biological diversity due to economic activities, climate change and its impacts on the agricultural and river basin systems, and other forms of crises owning to conflicts over access to shared resources. The *GMSARN International Journal* is dedicated to advance knowledge in energy, environment, natural resource management and economical development by the vigorous examination and analysis of theories and good practices, and to encourage innovations needed to establish a successful approach to solve an identified problem.

The *GMSARN International Journal* is a quarterly journal published by GMSARN in March, June, September and December of each year. Papers related to energy, environment, natural resource management, and economical development are published. The papers are reviewed by world renowned referees.

Preparation Guidelines

1. The manuscript should be written in English and the desired of contents is: Title, Author's name, affiliation, and address; Abstract, complete in itself and not exceeding 200 words; Text, divided into sections, each with a separate heading; Acknowledgments; References; and Appendices. The standard International System of Units (SI) should be used.

2. Illustrations (i.e., graphs, charts, drawings, sketches, and diagrams) should be submitted on separate sheets ready for direct reproduction. All illustrations should be numbered consecutively and given proper legends. A list of illustrations should be included in the manuscript. The font of the captions, legends, and other text in the illustrations should be Times New Roman. Legends should use capital letters for the first letter of the first word only and use lower case for the rest of the words. All symbols must be italicized, e.g., α, θ, Q_{wt}. Photographs should be black and white glossy prints; but good color photographs are acceptable.

3. Each reference should be numbered sequentially and these numbers should appear in square brackets in the text, e.g. [1], [2, 3], [4]–[6]. All publications cited in the text should be presented in a list of full references in the Reference section as they appear in the text (not in alphabetical order). Typical examples of references are as follows:

   - **Book references** should contain: name of author(s); year of publication; title; edition; location and publisher. Typical example: [2] Baker, P.R. 1978. Biogas for Cooking Stoves. London: Chapman and Hall.
   - **Journal references** should contains: name of author(s); year of publication; article title; journal name; volume; issue number; and page numbers. For example: Mayer, B.A.; Mitchell, J.W.; and El-Wakil, M.M. 1982. Convective heat transfer in veetrough liner concentrators. Solar Energy 28 (1): 33-40.
   - **Proceedings reference** example: [3] Mayer, A. and Biscaglia, S. 1989. Modelling and analysis of lead acid battery operation. Proceedings of the Ninth EC PV Solar Conference. Reiburg, Germany, 25-29 September. London: Kluwer Academic Publishers.
   - **Technical paper** reference example: [4] Mead, J.V. 1992. Looking at old photographs: Investigating the teacher tales that novice teachers bring with them. Report No. NCRTL-RR-92-4. East Lansing, MI: National Center for Research on Teacher Learning. (ERIC Document Reproduction Service No. ED346082).
   - **Online journal** reference example: [5] Tung, F. Y.-T., and Bowen, S. W. 1998. Targeted inhibition of hepatitis B virus gene expression: A gene therapy approach. Frontiers in Bioscience [On-line serial], 3. Retrieved February 14, 2005 from http://www.bioscience.org/1998/v3/a/tung/a11-15.htm.

4. Manuscript can be uploaded to the website or sent by email to gmsarn@ait.asia. In case of hard copy, three copies of the manuscript should be initially submitted for review. The results of the review along with the referees' comments will be sent to the corresponding author in due course. At the time of final submission, one copy of the manuscript and illustrations (original) should be submitted with the diskette. Please look at the author guide for detail.

GMSARN Members

Asian Institute of Technology

Guangxi University

Hanoi University of Technology

Ho Chi Minh City University of Technology

Institute of Technology of Cambodia

Khon Kaen University

Kunming University of Science and Technology

Nakhon Phanom University

National University of Laos

Royal University of Phnom Penh

Thammasat University

Ubon Ratchathani University

Yangon Technological University

Yunnan University

Associate Member

Mekong River Commission

Published by the

Greater Mekong Subregion Academic and Research Network (GMSARN)
c/o Asian Institute of Technology (AIT)
P.O. Box 4, Klong Luang
Pathumthani 12120, Thailand
Tel: (66-2) 524-6537; Fax: (66-2) 524-6589
E-mail: gmsarn@ait.ac.th
Website: http://www.gmsarn.com